Supporting Information

Kinetic Molecular Sieving, Thermodynamic and Structural Aspects of Gas/Vapor Sorption on Metal Organic Framework $[Ni_{1.5}(4,4'\text{-bipyridine})_{1.5}(H_3L)(H_2O)_3]\cdot[H_2O]_7$ where H_6L = 2,4,6-trimethylbenzene-1,3,5-triyl *tris*(methylene) triphosphonic acid.

Xuebo Zhao[1], Jon G. Bell[2], Si-fu Tang[3], Liangjun Li[1] and K Mark Thomas[2]

[1]Research Institute of Unconventional Petroleum and Renewable Energy, China University of Petroleum (East China), Qingdao 266580, P. R. China

[2]Wolfson Northern Carbon Reduction Laboratories, School of Chemical Engineering and Advanced Materials, Newcastle University, Newcastle upon Tyne, NE1 7RU, U.K.

[3]Key Laboratory of Biofuel, Chinese Academy of Sciences, Qingdao Institute of Bioenergy and Bioprocess Technology, Qingdao, Shandong 266101, P. R. China

Contents

Page

1. Synthesis of 2,4,6-trimethylbenzene-1,3,5-triyl *tris*(methylene) triphosphonic acid (H_6L). 3

2. Scanning Electron Microscopy 5

3 X-ray Crystallographic Studies 5

3.1 Single Crystal Data 5

3.2 Void Volume Data for the 'as-synthesized' and 'activated' samples of $[Ni_{1.5}(4,4'\text{-bipy})_{1.5}(H_3L)(H_2O)_3]$ 9

3.2 Powder X-ray Diffraction Studies 9

4. Infrared Spectroscopy 10

5. Thermogravimetric Studies 11

6. Gas/Vapor Adsorption Studies 12

6.1 Water Vapor Adsorption/Desorption Kinetics Profiles at 20°C 12

6.2 Ethanol Vapor Adsorption/desorption on $Ni_{1.5}(4,4'\text{-bipy})_{1.5}(H_3L)$ 15

6.2.1 Isosteric Enthalpy of Ethanol Adsorption

6.2.2 Ethanol Vapor Adsorption and DesorptionKinetic profiles 16

6.2.2.1 Adsorption/Desorption Kinetic Profiles at 20°C 16

6.2.2.2 Adsorption/Desorption Kinetic Profiles at 30°C 19

6.2.2.3 Adsorption/Desorption Kinetic Profiles at 40°C 22

6.2.2.4 Adsorption/Desorption Kinetic Profiles at 50°C 24

6.2.2.5 Variation of Ethanol Desorption Kinetic Parameters with Pressure 25

6.3 Carbon Dioxide Adsorption 28

6.3.1 Virial Graphs 28

6.3.2 Enthalpy of Adsorption at Zero Surface Coverage 31

6.3.3 Typical Carbon Dioxide Adsorption Kinetic Profiles 32

6.3.3.1 Carbon Dioxide Kinetic Profiles for Adsorption at 30°C 32

6.3.3.2 Carbon Dioxide Kinetic Profiles for Adsorption at 45°C 33

6.3.3.3 Carbon Dioxide Kinetic Profiles for Adsorption at 60°C 35

6.3.3.4 Carbon Dioxide Kinetic Profiles for Adsorption at 75°C 36

6.3.4 Activation Energy Graphs for CO_2 Adsorption on $[Ni_{1.5}(4,4'\text{bipy})_{1.5}(H_3L)]$ 38

References 39

Supporting information

1. Synthesis of 2,4,6-trimethylbenzene-1,3,5-triyl *tris*(methylene)triphosphonic acid (H_6L).

The ligand was synthesized by reacting *tris*(bromomethyl)mesitylene[1] with triethylphosphite (Aldrich) and followed by refluxing the obtained oil with conc. hydrochloric acid according to the literature method[2,3]. Block colorless crystals were obtained from the water solution by slow evaporation.

^{1}H NMR ($CDCl_3$) data for *tris*(bromomethyl)mesitylene: δ 2.39 (**H**$_3$C-Ar, s, 9H); 4.50 (Br-C**H**$_2$-Ar, d, 6H).

^{1}H NMR (D_2O) data for H_6L: δ 2.397 (**H**$_3$C-, s, 9H); 3.373, 3.409 (P-C**H**$_2$-, d, 6H). IR(KBr, cm^{-1}): 3300.2 (s, br), 2923.7 (m, br), 2278.6 (w, br), 1835.0 (w), 1635.9 (m), 1422.3 (w), 1385.7 (vw), 1254.0 (m), 1233.3 (m), 1188.9 (s), 1137.4 (s), 1061.7(m), 1016.4 (s), 994.2 (s), 954.2 (s), 922.8 (s), 870.3 (m, 851.5 (m), 773.8 (w), 747.8 (m), 646.1 (w), 631.1 (m), 573.7 (w), 558.3 (vw), 520.2 (s), 507.2 (m), 451.3 (m), 427.7 (m). Elemental analysis (%) calcd for $H_6L{\cdot}H_2O$ ($C_{12}H_{23}O_{10}P_3$): C 34.30, H 5.52; found: C 34.34, H 5.42.

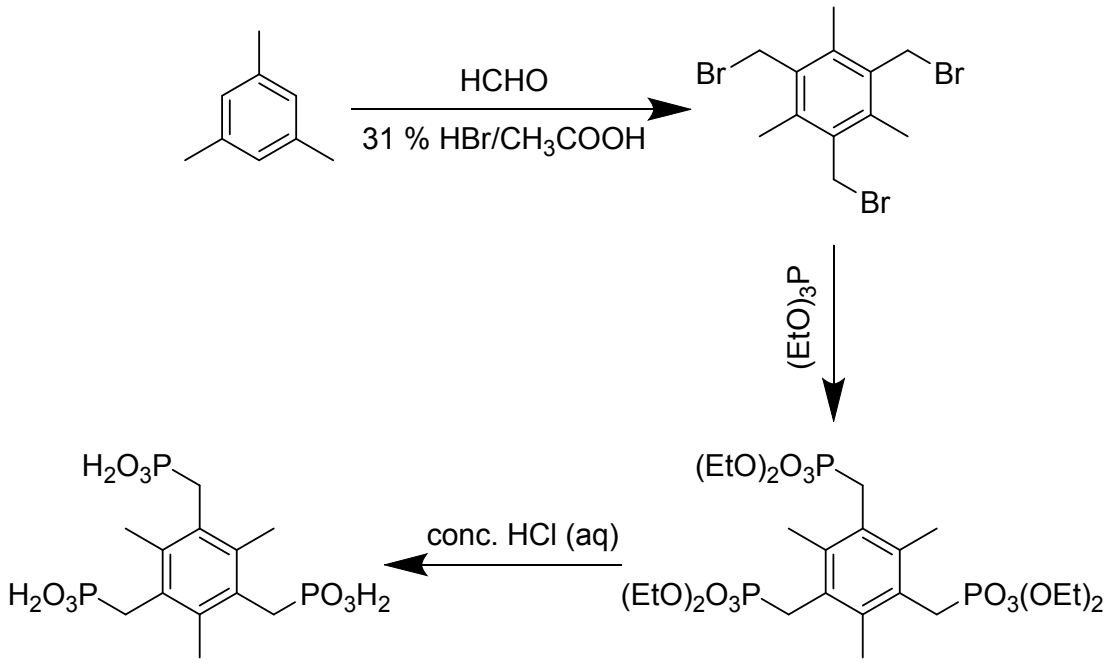

Scheme 1. Synthesis procedure of 2,4,6-trimethylbenzene-1,3,5-triyl

tris(methylene)triphosphonic acid

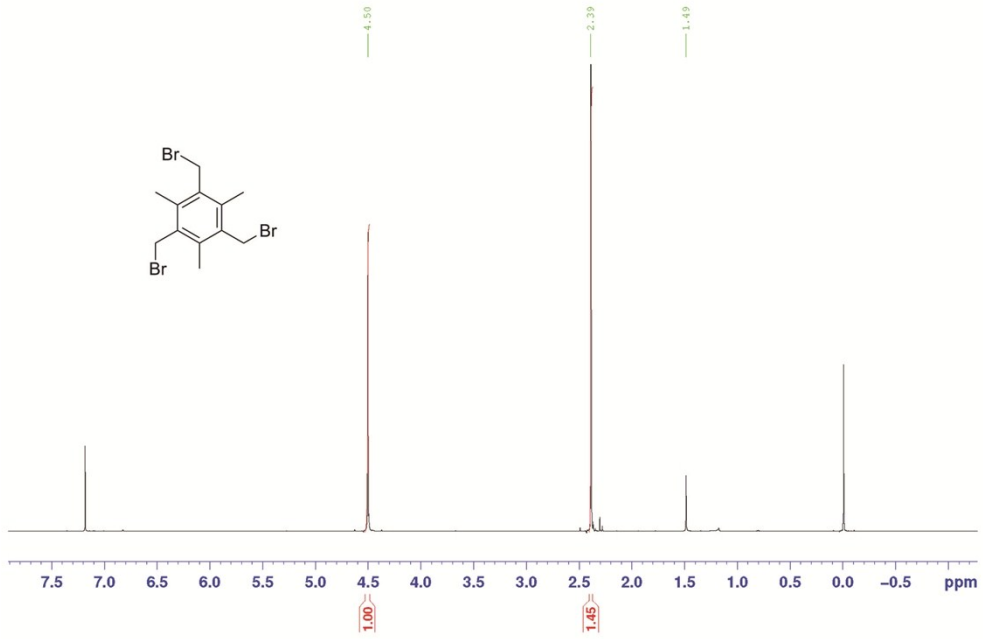

Figure S1. ^{1}H NMR spectrum of *tris(*bromomethyl)mesitylene.

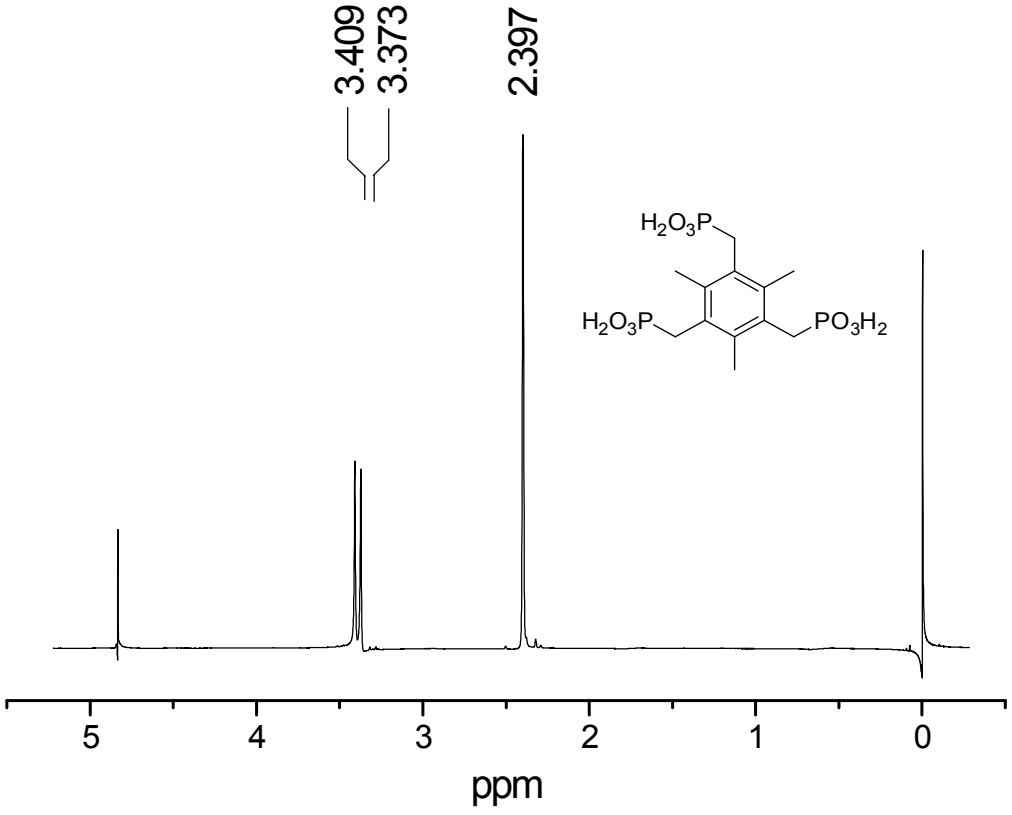

Figure S2. ^{1}H NMR spectrum of H_6L.

2. Scanning Electron Microscopy

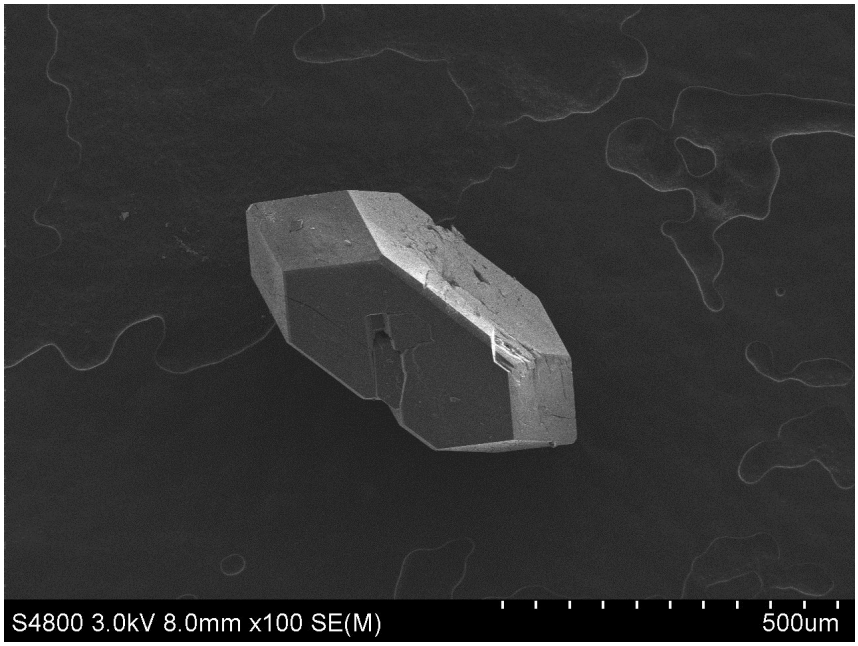

Figure S3. SEM image of a crystal of $[Ni_{1.5}(4,4'\text{-bipy})_{1.5}(H_3L)(H_2O)_3]\cdot[H_2O]_7$.

3. X-ray Crystallographic Studies

3.1 Single Crystal Data

Table S1. Selected bond lengths (Å)

RT		110 °C	
Ni(1)-O(4)	2.078(5)	Ni(1)-O(4)#1	2.086(3)
Ni(1)-O(4)#1	2.078(5)	Ni(1)-O(4)	2.086(3)
Ni(1)-O(4)#2	2.078(5)	Ni(1)-O(4)#2	2.086(3)
Ni(1)-O(4)#3	2.078(5)	Ni(1)-O(4)#3	2.086(3)
Ni(1)-N(1)	2.169(11)	Ni(1)-N(1)#3	2.158(6)
Ni(1)-N(1)#2	2.169(11)	Ni(1)-N(1)	2.158(6)
Ni(2)-O(1)	1.989(18)	Ni(2)-O(1)	2.053(9)
Ni(2)-O(2W)	2.069(11)	Ni(2)-O(2W)	2.078(7)
Ni(2)-N(2)#4	2.099(10)	Ni(2)-N(2)#4	2.084(6)
Ni(2)-N(2)	2.099(10)	Ni(2)-N(2)	2.084(6)
Ni(2)-O(1W)	2.109(8)	Ni(2)-O(1W)	2.086(5)
Ni(2)-O(1W)#4	2.109(8)	Ni(2)-O(1W)#4	2.086(5)

Symmetry transformations used to generate equivalent atoms: #1 -x+1,-y,z; #2 y+1/2,-x+1/2,-z+1/2; #3 -y+1/2,x-1/2,-z+1/2; #4 -y+1,-x+1,z.

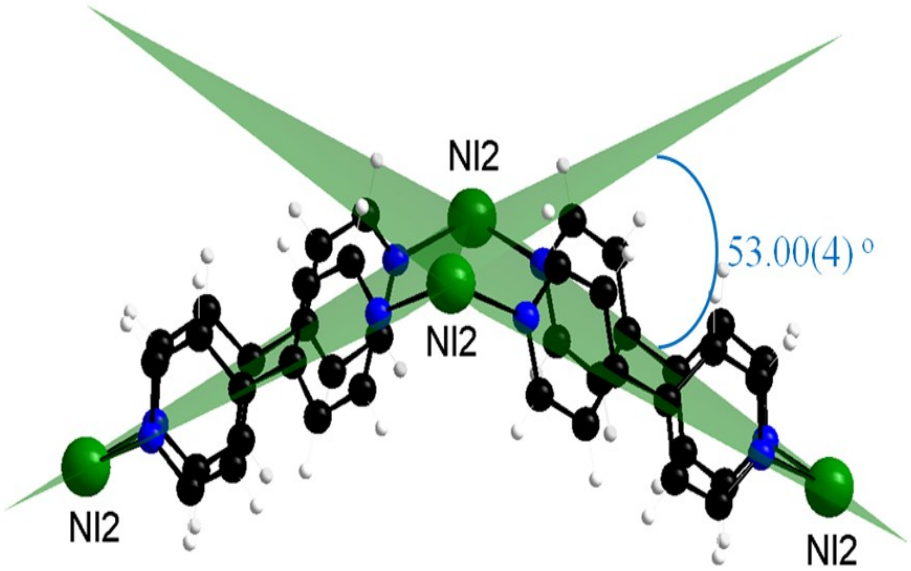

Figure S4. $[Ni(4,4'\text{-bipy})]_4$ distorted circle view through *c*-axis. One Ni2 atom is about 6.6838 Å out of the plane defined by another three, the dihedral angle between these two planes is about 53.00(4) º.

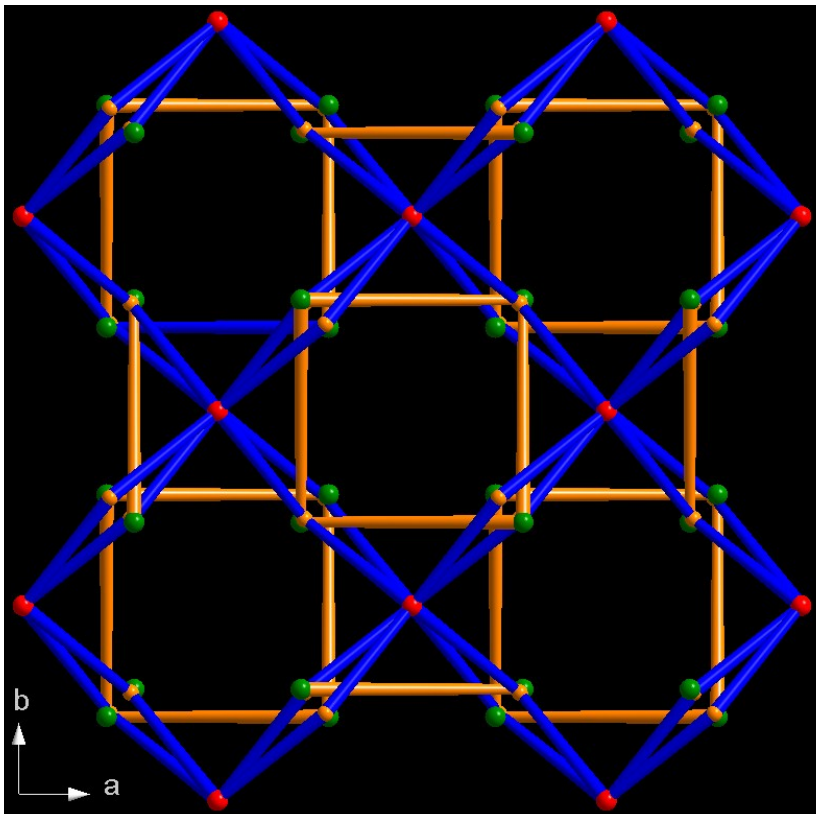

Figure S5. Topology schematic diagram of compound $[Ni_{1.5}(4,4'\text{-bipy})_{1.5}(H_3L)(H_2O)_3]$. Triphosphonate ligand, Ni1 and Ni2 are represented as brown,

red and brown balls, respectively.

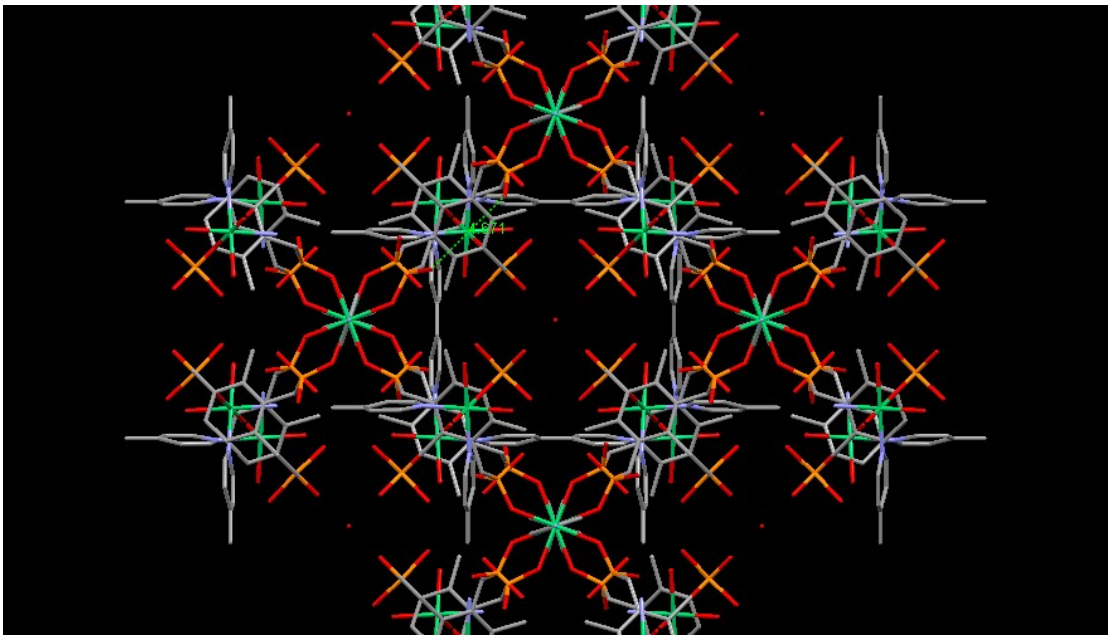

View down *c*-axis

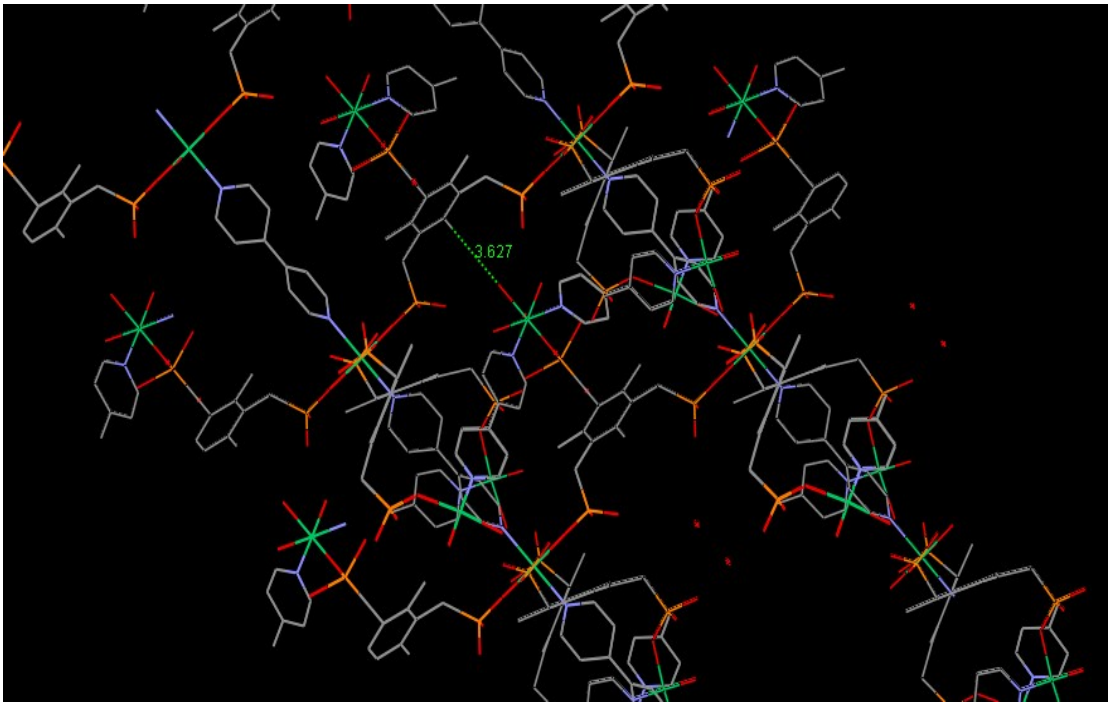

View down *a*-axis+45

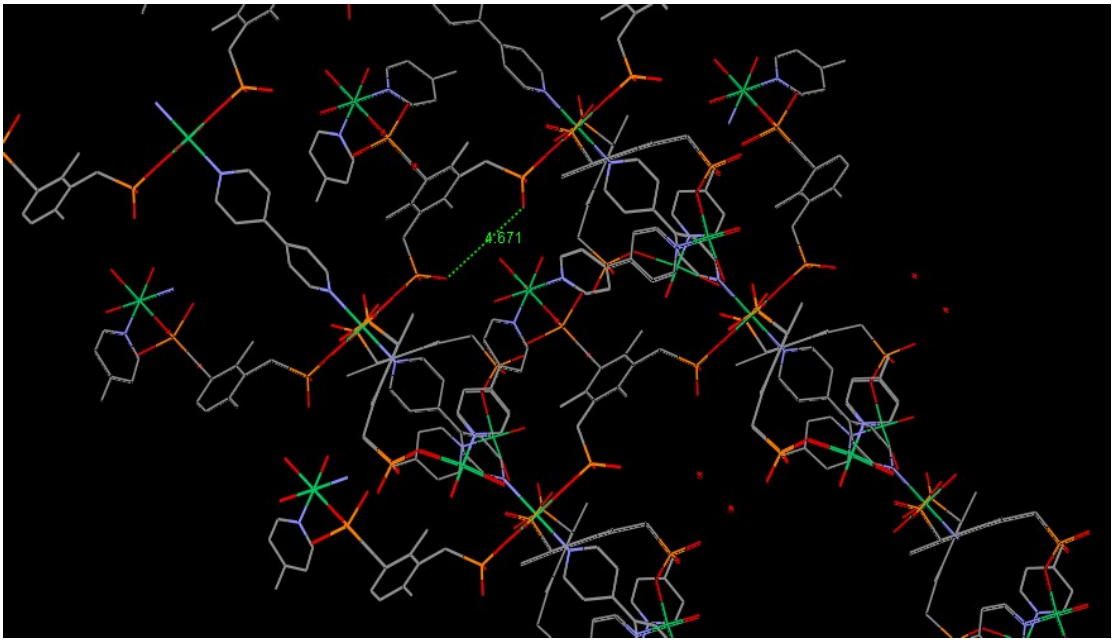

View down *a*-axis+45

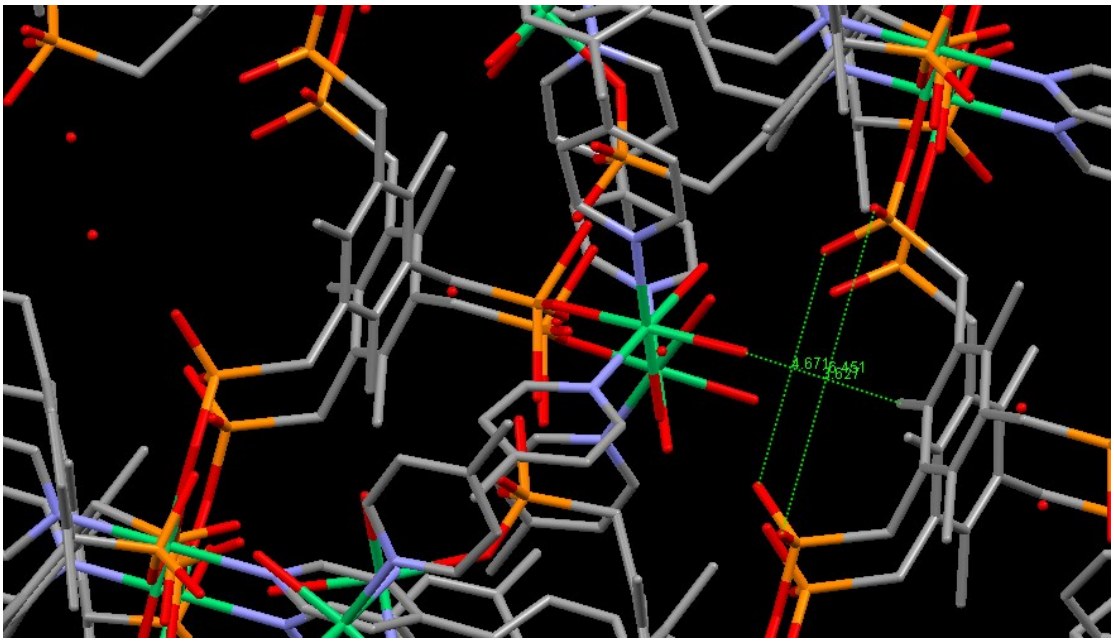

Figure S6 Schematic diagrams of structure of $[Ni_{1.5}(4,4'\text{-bipy})_{1.5}(H_3L)(H_2O)_3]$. Views down c axis and a-axis+45 showing narrow pore windows (size 4.671 x 3.627A and 6.451 x 3.627A).

3.2 Void Volume Data for the 'as-synthesized' and 'activated' samples of $[Ni_{1.5}(4,4'\text{-bipy})_{1.5}(H_3L)(H_2O)_3]$

Table S2. Pore volume Data calculated from Crystallographic Data using Platon

	Remove lattice water		Remove both lattice and coordinated water	
$[Ni_{1.5}(4,4'\text{-bipy})_{1.5}(H_3L)(H_2O)_3]\cdot[H_2O]_7$	25.4% (v/v)	0.1946 $cm^3\ g^{-1}$	28.4% (v/v)	0.2327 $cm^3\ g^{-1}$
$[Ni_{1.5}(4,4'\text{-bipy})_{1.5}(H_3L)(H_2O)_3]$ [activated at 110°C in vacuum	25.6% (v/v)	0.1962 $cm^3\ g^{-1}$	28.8% (v/v)	0.2360 $cm^3\ g^{-1}$

3.3 Powder X-ray Diffraction Data

(a)

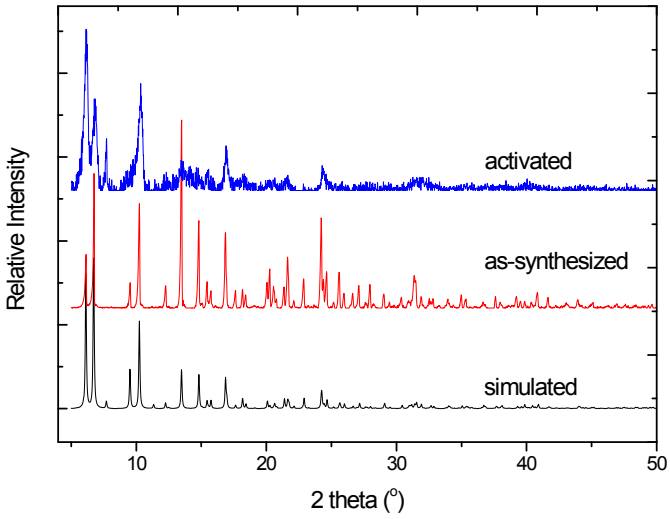

(b)

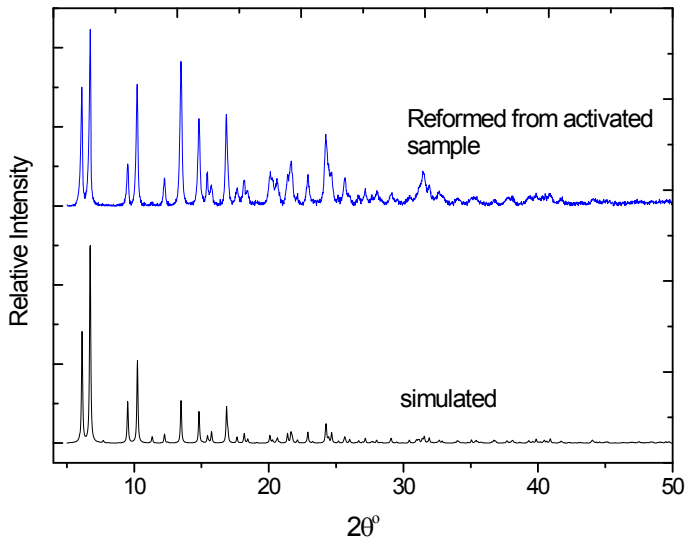

Figure S7. PXRD profiles (a) comparison of $[Ni_{1.5}(4,4'\text{-bipy})_{1.5}(H_3L)(H_2O)_3]\cdot[H_2O]_7$, sample activated at 110°C in vacuum ($[Ni_{1.5}(4,4'\text{-bipy})_{1.5}(H_3L)(H_2O)_3]$ and simulated from the crystal structure and (b) showing reformation $[Ni_{1.5}(4,4'\text{-bipy})_{1.5}(H_3L)(H_2O)_3]\cdot[H_2O]_7$ from activated sample and simulated profile.

4. Infrared Spectroscopy

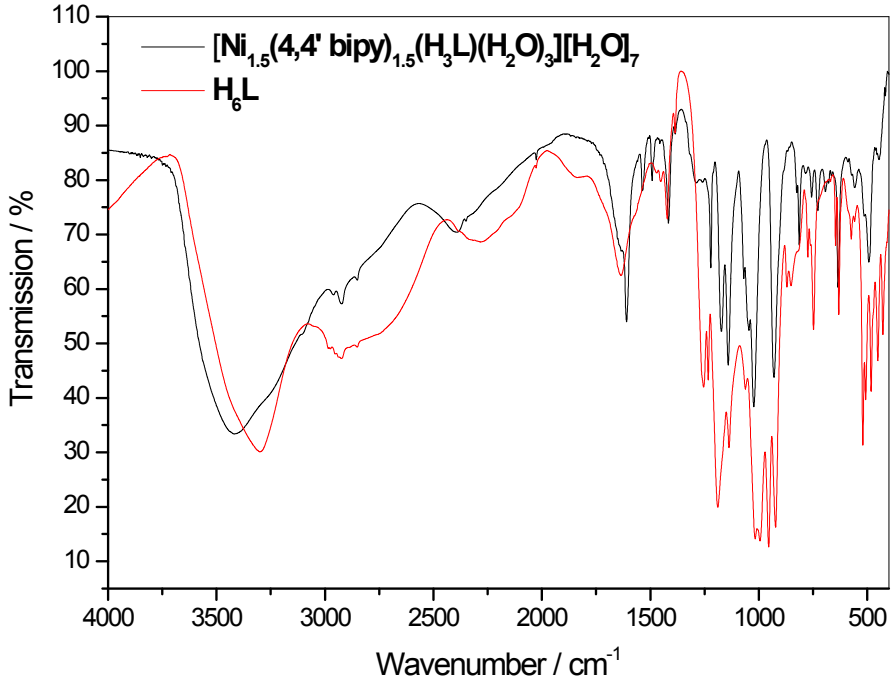

Figure S8. IR spectra of compound $[Ni_{1.5}(4,4'\text{-bipy})_{1.5}(H_3L)(H_2O)_3][H_2O]_7$ and H_6L.

5. Thermogravimetric Analysis(TGA)

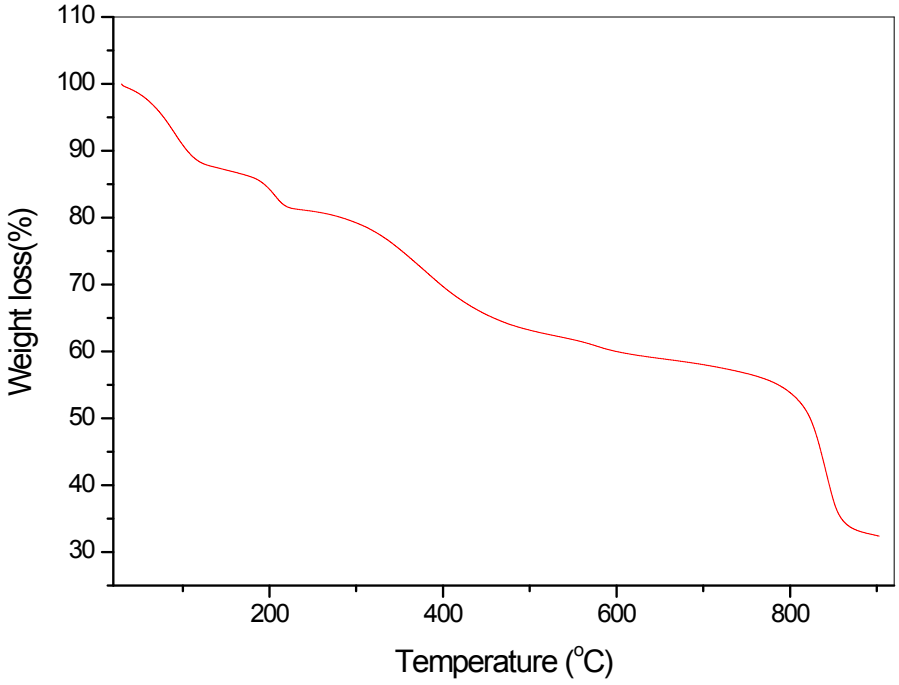

Figure S9. TGA profile for $[Ni_{1.5}(4,4'\text{-bipy})_{1.5}(H_3L)(H_2O)_3]\cdot[H_2O]_7$.

6. Gas/Vapor Adsorption Studies

6.1 Water Vapor Adsorption/desorption Kinetics Profiles at 20°C

(a)

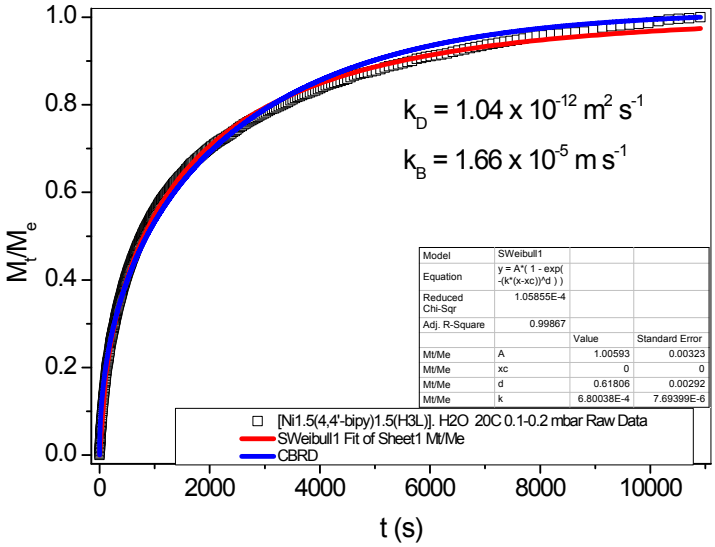

(b)

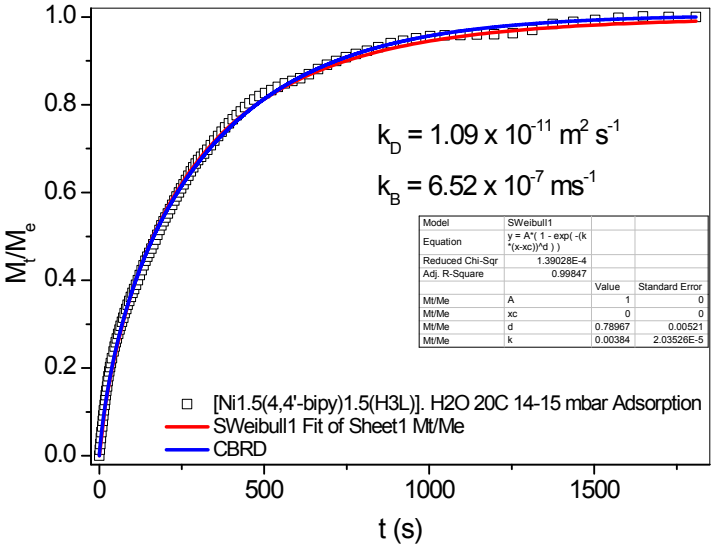

(c)

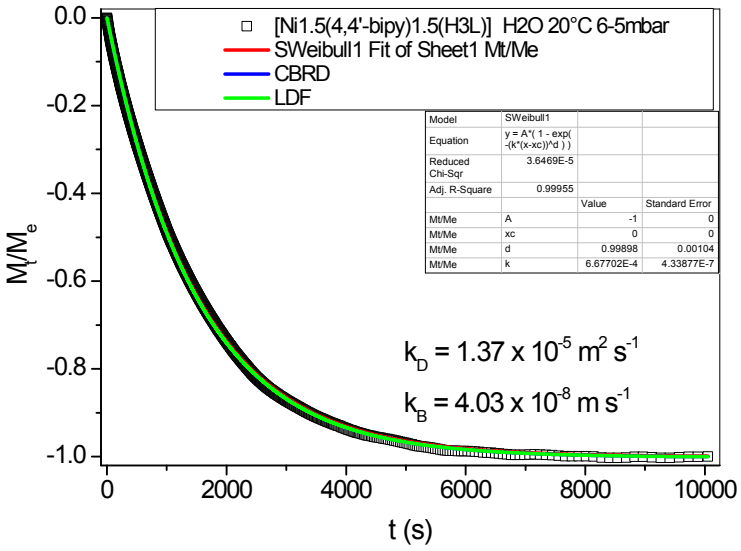
[Ni1.5(4,4'-bipy)1.5(H3L)] H2O 20°C 6-5mbar
SWeibull1 Fit of Sheet1 Mt/Me
CBRD
LDF
Model SWeibull1
Equation y = A*(1 - exp(-(k*(x-xc))^d))
Reduced Chi-Sqr 3.6469E-5
Adj. R-Square 0.99955
Value Standard Error
Mt/Me A -1 0
Mt/Me xc 0 0
Mt/Me d 0.99898 0.00104
Mt/Me k 6.67702E-4 4.33877E-7
k_D = 1.37 x 10^{-5} m^2 s^{-1}
k_B = 4.03 x 10^{-8} m s^{-1}
M_t/M_e
t (s)

(d)

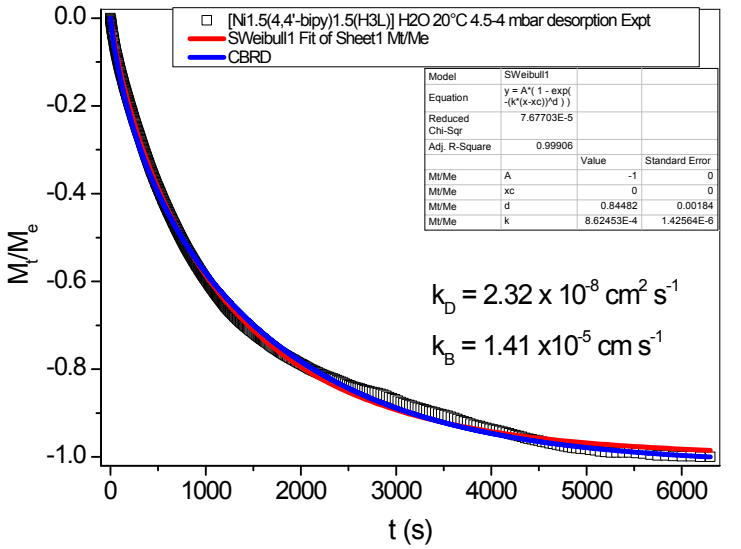
[Ni1.5(4,4'-bipy)1.5(H3L)] H2O 20°C 4.5-4 mbar desorption Expt
SWeibull1 Fit of Sheet1 Mt/Me
CBRD
Model SWeibull1
Equation y = A*(1 - exp(-(k*(x-xc))^d))
Reduced Chi-Sqr 7.67703E-5
Adj. R-Square 0.99906
Value Standard Error
Mt/Me A -1 0
Mt/Me xc 0 0
Mt/Me d 0.84482 0.00184
Mt/Me k 8.62453E-4 1.42564E-6
k_D = 2.32 x 10^{-8} cm^2 s^{-1}
k_B = 1.41 x10^{-5} cm s^{-1}
M_t/M_e
t (s)

(e)

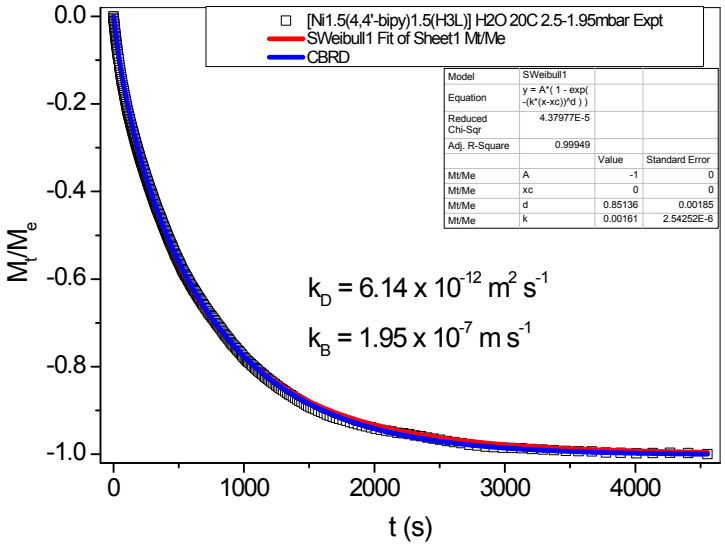

Figure S10. Water Vapor Adsorption and Desorption Kinetic Profiles for $[Ni_{1.5}(4,4'\ bipy)_{1.5}(H_3L)]$ at 20°C, (a) Pressure Increment 0.1-0.2 mbar, (b) Pressure Increment 14-15 mbar, (c) Pressure Decrement 6-5 mbar, (d) Pressure Decrement 4.5-4 mbar, (e) Pressure Decrement 2.5-1.95 mbar

6.2 Ethanol Vapor Adsorption/Desorption on $Ni_{1.5}(4,4'\text{-bipy})_{1.5}(H_3L)$

6.2.1 Isosteric Enthalpy of Ethanol Adsorption

(a)

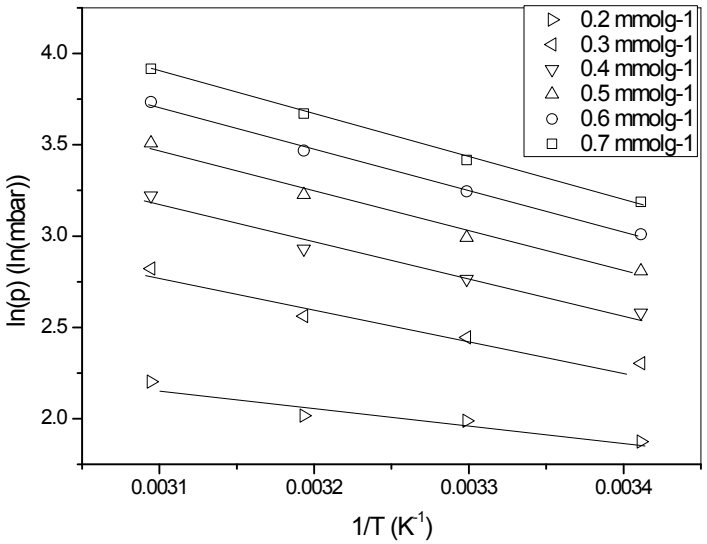

(b)

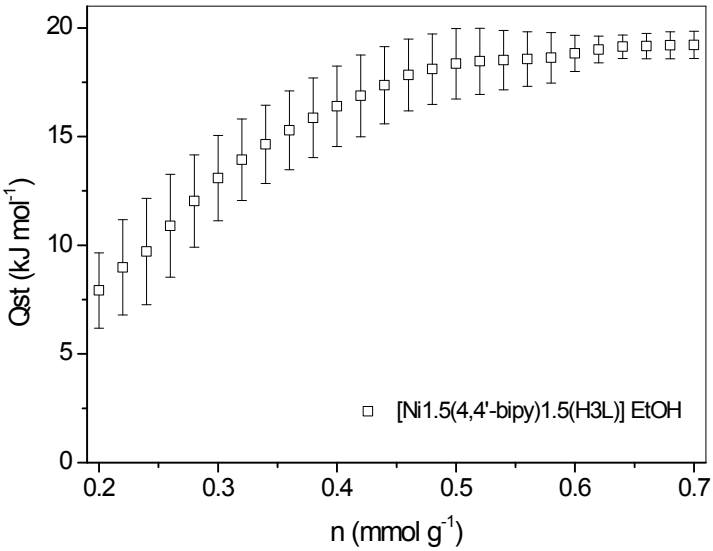

Figure S11 Adsorption of Ethanol Vapor on $[Ni_{1.5}(4,4'\text{ bipy})_{1.5}(H_3L)]$ (a) Graphs of ln(p) versus 1/T and (b) The Variation of $Q_{st,n}$ with amount adsorbed

6.2.2 Ethanol Vapor Adsorption and Desorption Kinetic Profiles

6.2.2.1Adsorption/Desorption Kinetic Profiles at 20°C

(a)

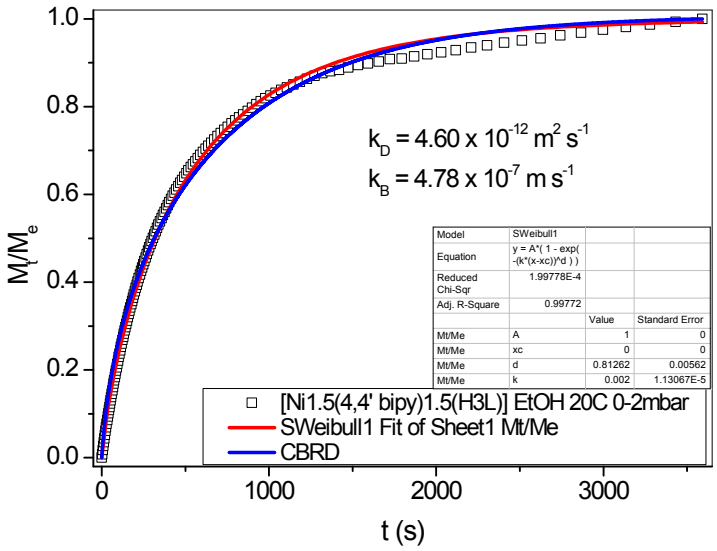

(b)

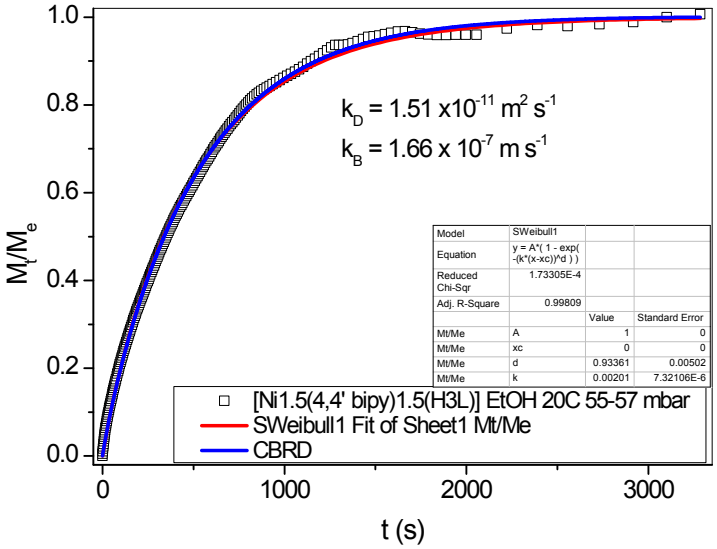

(c)

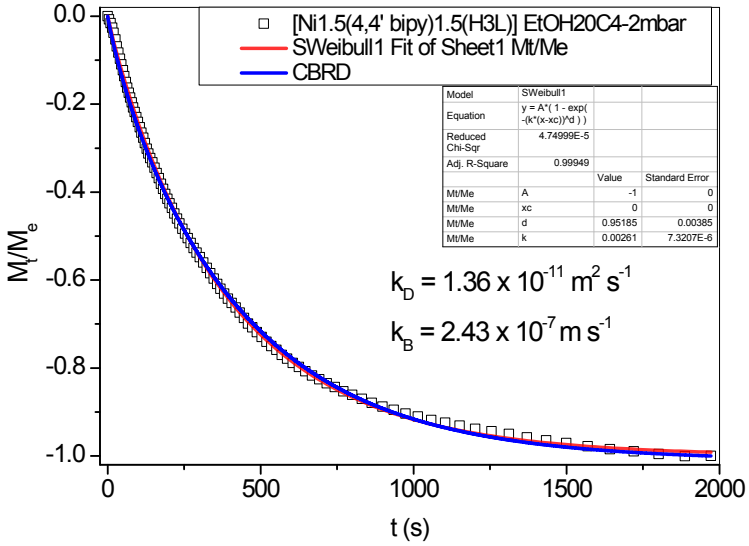
[Ni1.5(4,4' bipy)1.5(H3L)] EtOH20C4-2mbar
SWeibull1 Fit of Sheet1 Mt/Me
CBRD
Model SWeibull1
Equation y = A*(1 - exp(-(k*(x-xc))^d))
Reduced Chi-Sqr 4.74999E-5
Adj. R-Square 0.99949
Value Standard Error
Mt/Me A -1 0
Mt/Me xc 0 0
Mt/Me d 0.95185 0.00385
Mt/Me k 0.00261 7.3207E-6
$k_D = 1.36 \times 10^{-11}$ m^2 s^{-1}
$k_B = 2.43 \times 10^{-7}$ m s^{-1}
M_t/M_e
t (s)

(d)

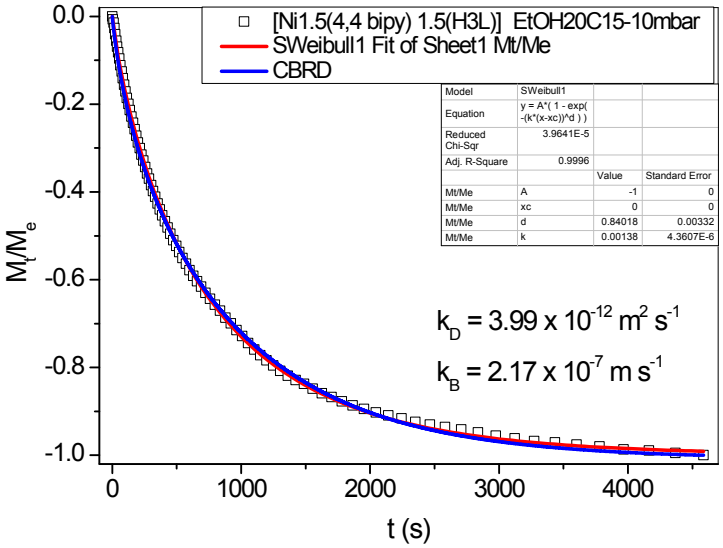
[Ni1.5(4,4 bipy) 1.5(H3L)] EtOH20C15-10mbar
SWeibull1 Fit of Sheet1 Mt/Me
CBRD
Model SWeibull1
Equation y = A*(1 - exp(-(k*(x-xc))^d))
Reduced Chi-Sqr 3.9641E-5
Adj. R-Square 0.9996
Value Standard Error
Mt/Me A -1 0
Mt/Me xc 0 0
Mt/Me d 0.84018 0.00332
Mt/Me k 0.00138 4.3607E-6
$k_D = 3.99 \times 10^{-12}$ m^2 s^{-1}
$k_B = 2.17 \times 10^{-7}$ m s^{-1}
M_t/M_e
t (s)

(e)

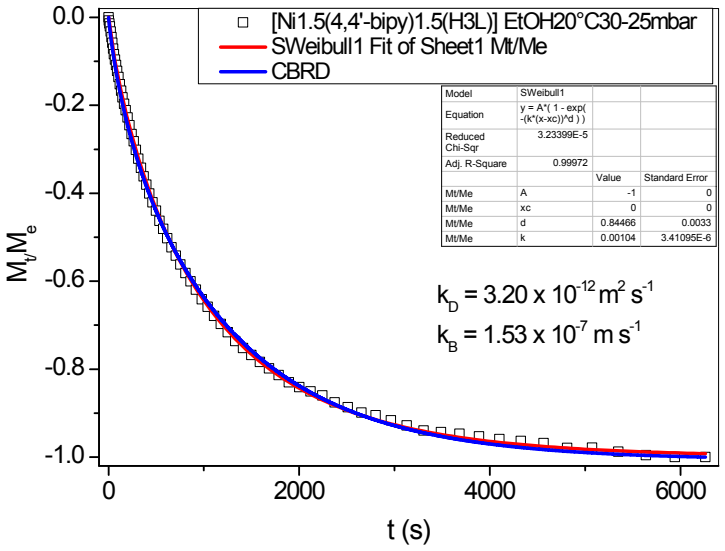

(f)

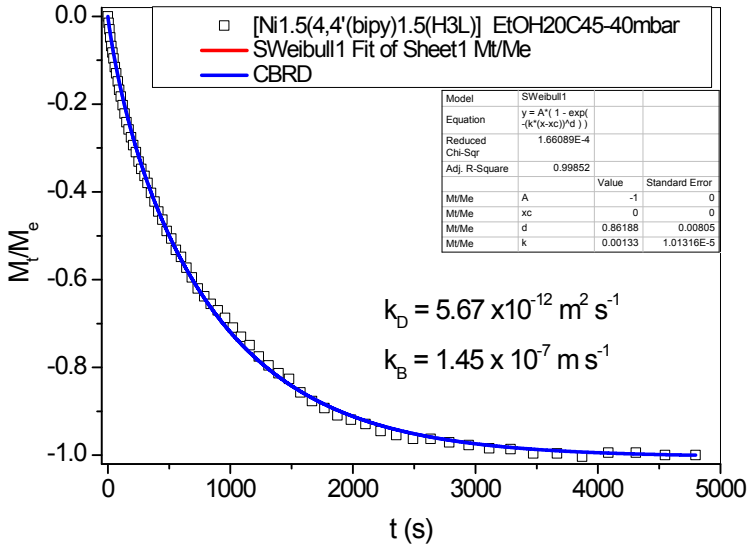

+

Figure S12. Ethanol Vapor Adsorption and Desorption Kinetic Profiles for $[Ni_{1.5}(4,4'\text{ bipy})_{1.5}(H_3L)]$ at 20°C, (a) Pressure Increment 0-2 mbar, (b) Pressure Increment 55-57 mbar, (c) Pressure Decrement 4-2 mbar, (d) Pressure Decrement 15-10 mbar, (e) Pressure Decrement 30-25 mbar, (f) Pressure Decrement 45-40 mbar.

6.2.2.2Adsorption/Desorption Kinetic Profiles at 30°C

(a)

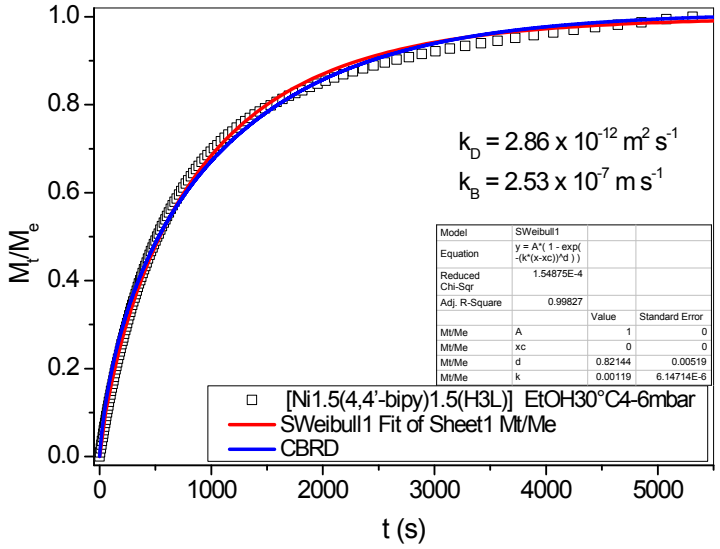

(b)

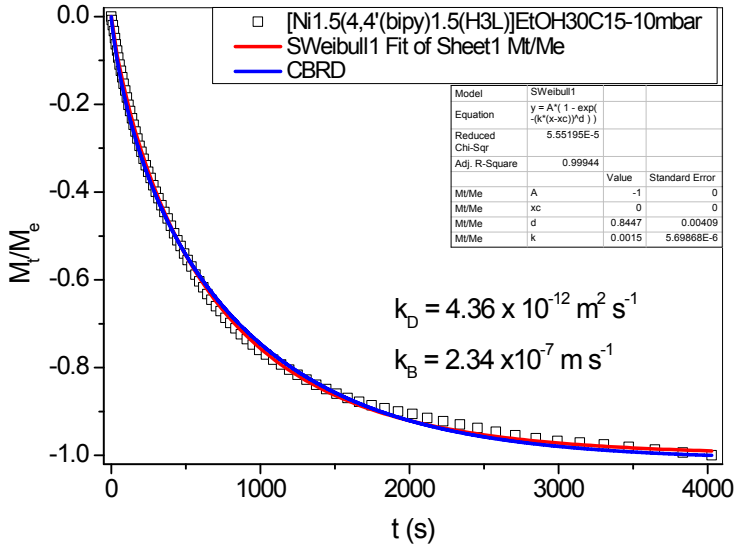

(c)

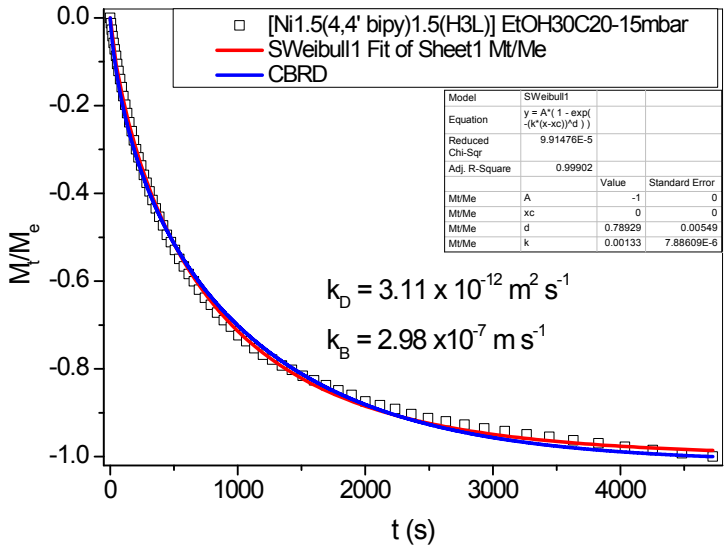
[Ni1.5(4,4' bipy)1.5(H3L)] EtOH30C20-15mbar
SWeibull1 Fit of Sheet1 Mt/Me
CBRD
Model SWeibull1
Equation y = A*(1 - exp(-(k*(x-xc))^d))
Reduced Chi-Sqr 9.91476E-5
Adj. R-Square 0.99902
Value Standard Error
Mt/Me A -1 0
Mt/Me xc 0 0
Mt/Me d 0.78929 0.00549
Mt/Me k 0.00133 7.88609E-6
$k_D = 3.11 \times 10^{-12}\ m^2\ s^{-1}$
$k_B = 2.98 \times 10^{-7}\ m\ s^{-1}$
M_t/M_e
t (s)

(d)

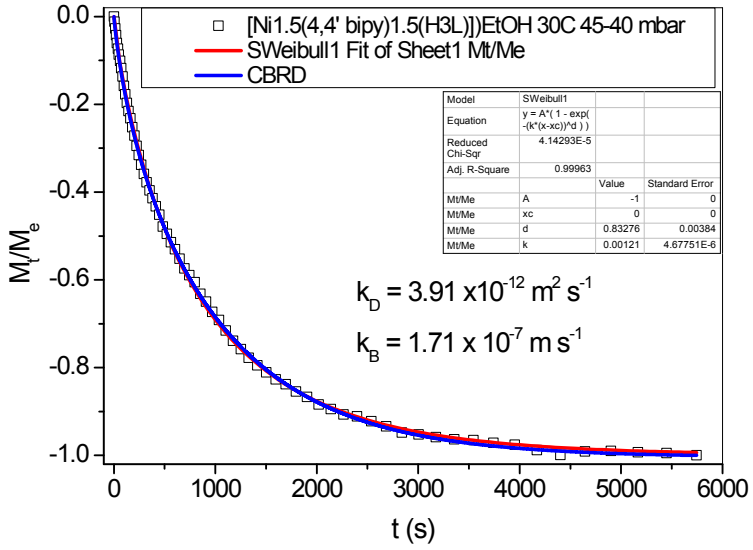
[Ni1.5(4,4' bipy)1.5(H3L)])EtOH 30C 45-40 mbar
SWeibull1 Fit of Sheet1 Mt/Me
CBRD
Model SWeibull1
Equation y = A*(1 - exp(-(k*(x-xc))^d))
Reduced Chi-Sqr 4.14293E-5
Adj. R-Square 0.99963
Value Standard Error
Mt/Me A -1 0
Mt/Me xc 0 0
Mt/Me d 0.83276 0.00384
Mt/Me k 0.00121 4.67751E-6
$k_D = 3.91 \times 10^{-12}\ m^2\ s^{-1}$
$k_B = 1.71 \times 10^{-7}\ m\ s^{-1}$
M_t/M_e
t (s)

(e)

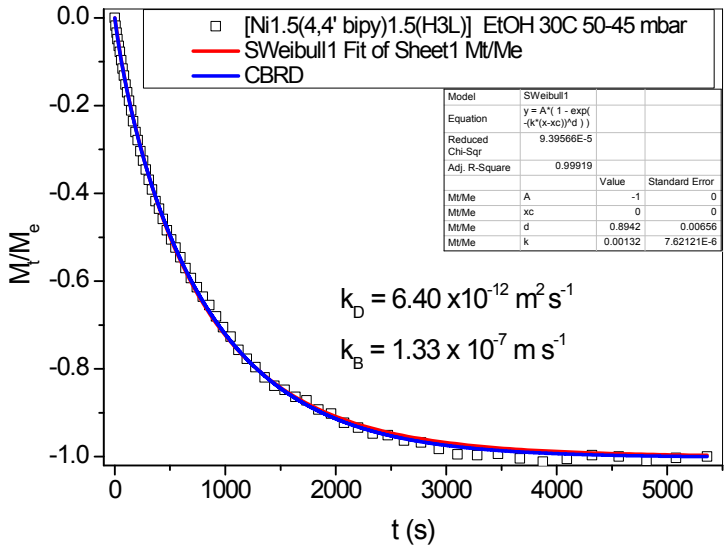

Figure S13. Ethanol Vapor Adsorption and Desorption Kinetic Profiles on $[Ni_{1.5}(4,4'\ bipy)_{1.5}(H_3L)]$ at 30°C, (a) Pressure Increment 4-6 mbar (b) Pressure Decrements 15-10 mbar, (c) Pressure Decrements 20-15 mbar, (d) Pressure Decrements 45-40 mbar, (e) Pressure Decrements 50-45 mbar.

6.2.2.3 Adsorption/Desorption Kinetic Profiles at 40°C

(a)

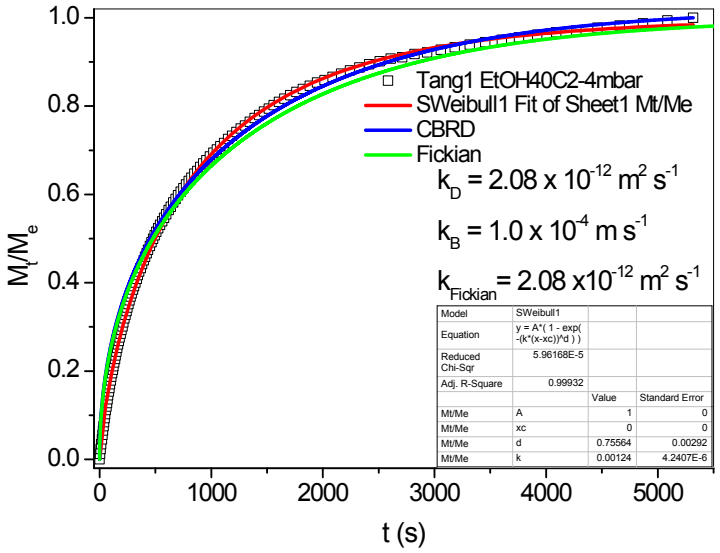

(b)

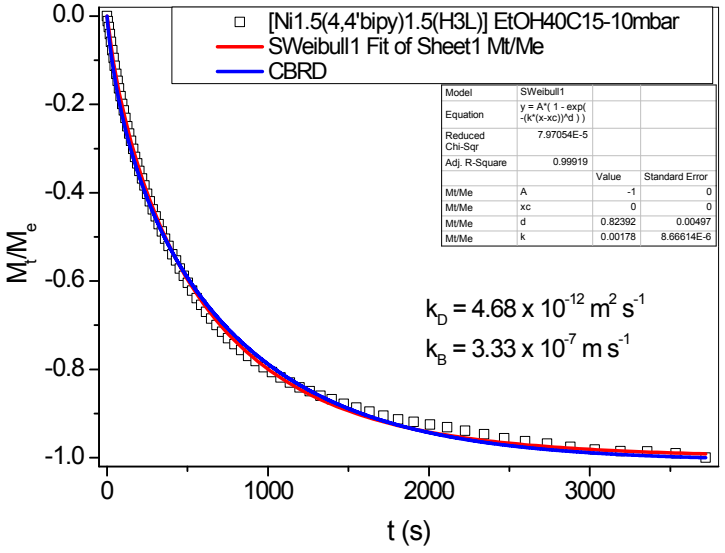

(c)

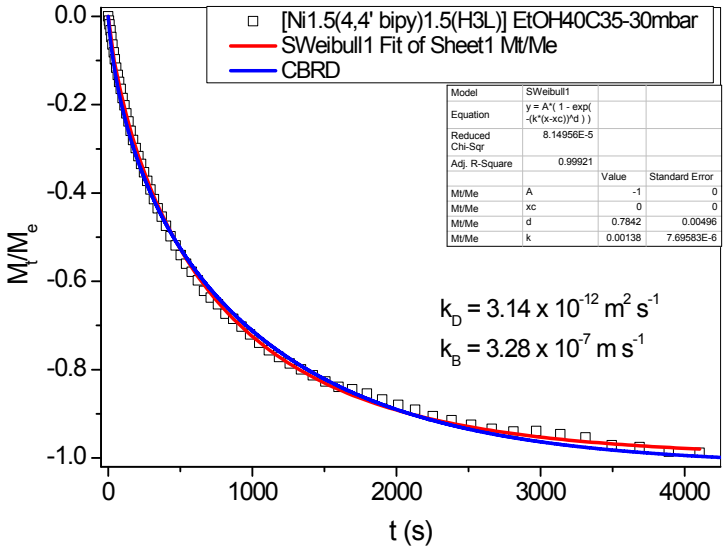

(d)

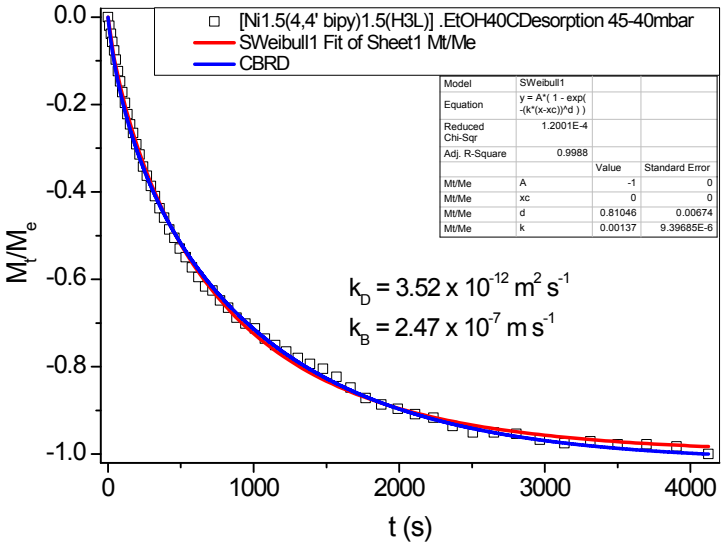

Figure S14. Ethanol Vapor Adsorption and Desorption Kinetic Profiles on [$Ni_{1.5}$(4,4' bipy)$_{1.5}$(H_3L)] at 40°C for , (a) Pressure Increment 2-4 mbar, (b) Pressure Decrement 15-10 mbar, (c) Pressure Decrement 35-30 mbar, (d) Pressure Decrement 45-40 mbar.

6.2.2.4 Adsorption/Desorption Kinetic Profiles at 50°C

(a)

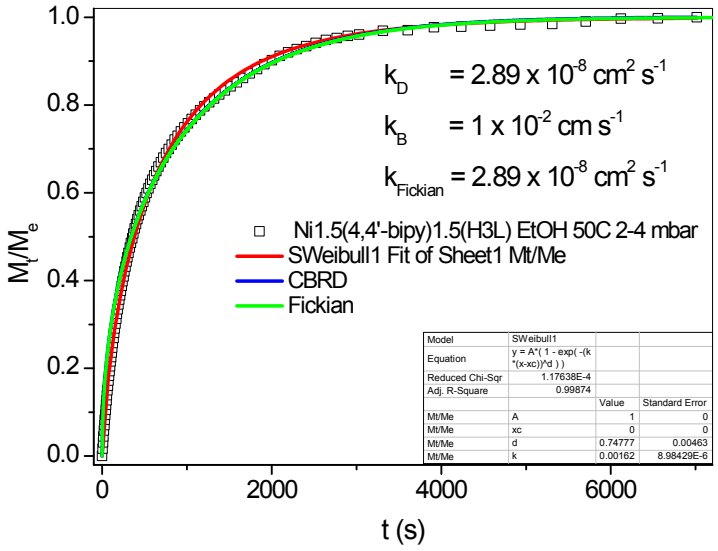

(b)

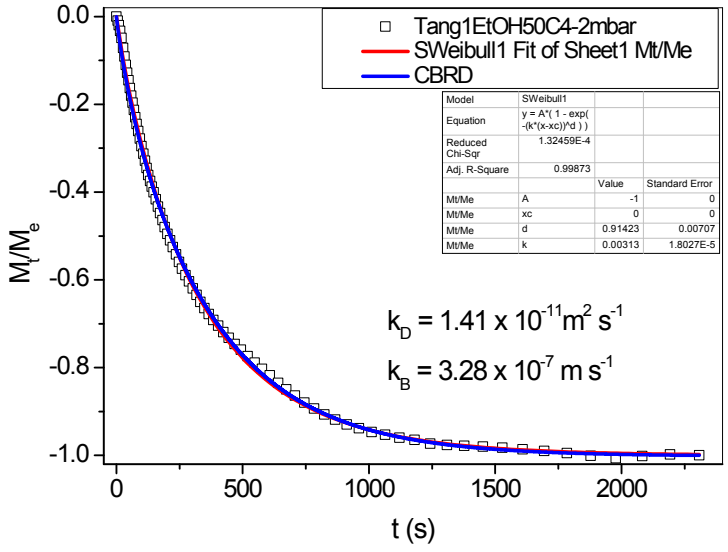

Figure S15. Ethanol Vapor Adsorption and Desorption Kinetic Profiles on $[Ni_{1.5}(4,4'\text{-bipy})_{1.5}(H_3L)]$ at 50°C, (a) Pressure Increment 2-4 mbar, (b) Pressure Decrement 4-2 mbar

6.2.2.5 Variation of Ethanol Desorption parameters with Pressure

(a)

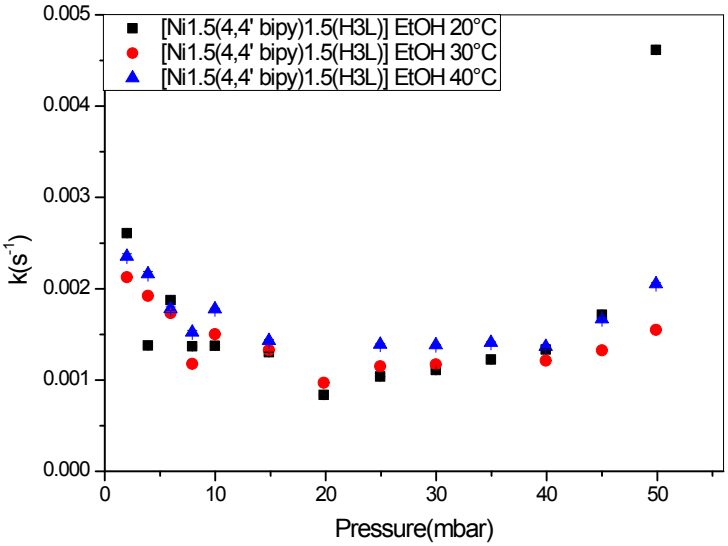

(b)

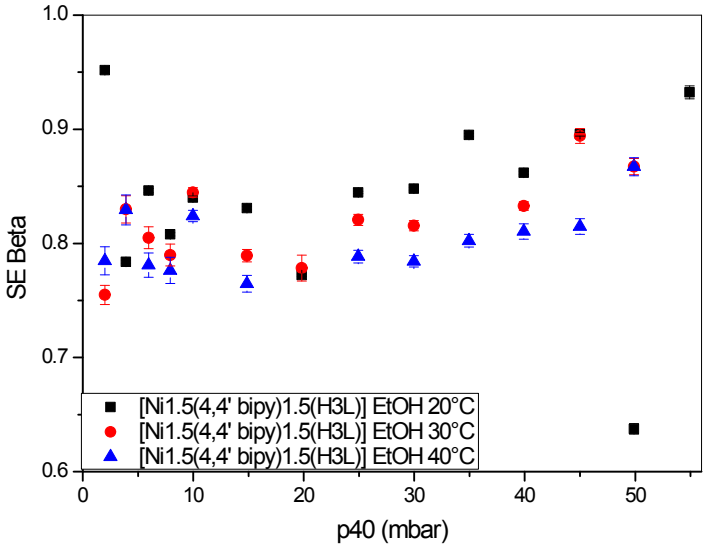

(c)

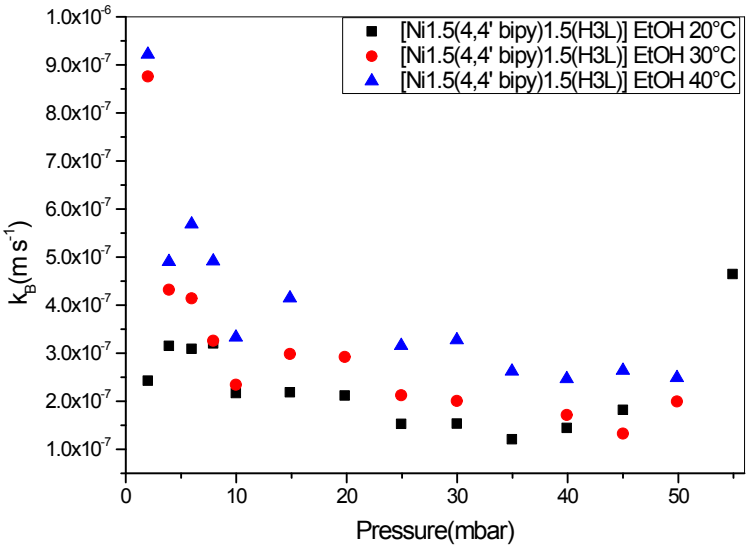
[Ni1.5(4,4' bipy)1.5(H3L)] EtOH 20°C
[Ni1.5(4,4' bipy)1.5(H3L)] EtOH 30°C
[Ni1.5(4,4' bipy)1.5(H3L)] EtOH 40°C
1.0x10-6
9.0x10-7
8.0x10-7
7.0x10-7
6.0x10-7
5.0x10-7
4.0x10-7
3.0x10-7
2.0x10-7
1.0x10-7
kB(m s-1)
0
10
20
30
40
50
Pressure(mbar)

(d)

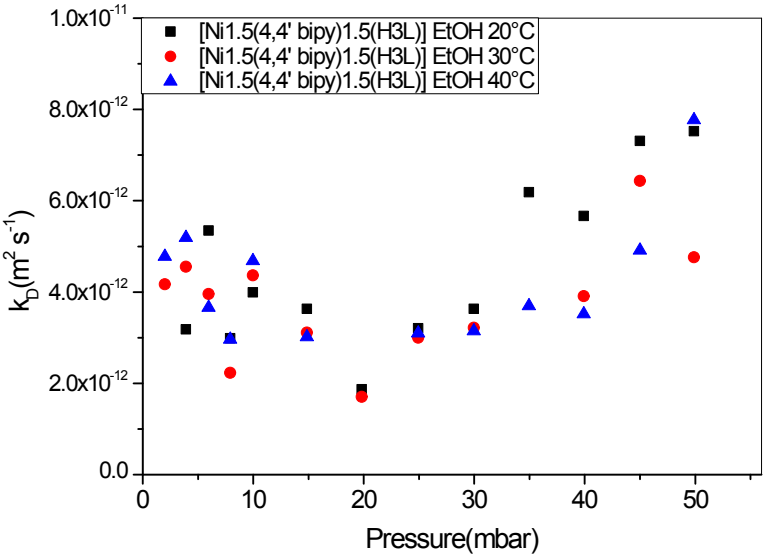
[Ni1.5(4,4' bipy)1.5(H3L)] EtOH 20°C
[Ni1.5(4,4' bipy)1.5(H3L)] EtOH 30°C
[Ni1.5(4,4' bipy)1.5(H3L)] EtOH 40°C
1.0x10-11
8.0x10-12
6.0x10-12
4.0x10-12
2.0x10-12
0.0
kD(m2 s-1)
0
10
20
30
40
50
Pressure(mbar)

(e)

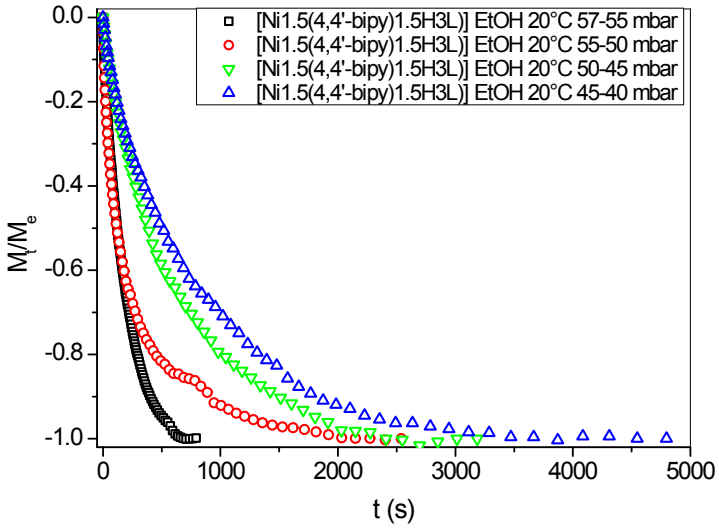

(f)

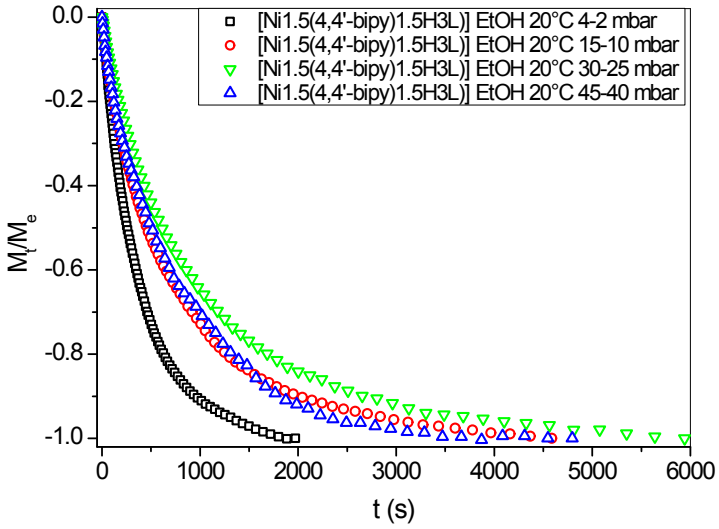

Figure S16. The variation of Kinetic Parameters for Ethanol Vapor Desorption on $[Ni_{1.5}(4,4'bipy)_{1.5}(H_3L)]$ with Pressure, Temperature and Loading (a) SE kinetic rate constant versus pressure (20-40°C), (b) SE Exponent (β) versus pressure (20-40°C),(c) CBRD k_B versus pressure (20-40°C), (d) CBRD k_D versus pressure (20-40°C), (e) Desorption kinetic profiles at 20°C for vapor pressure range 55-40 mbar and (f) Desorption kinetic profiles at 20°C for vapor pressure range 40-2 mbar.

6.3 Carbon Dioxide Adsorption

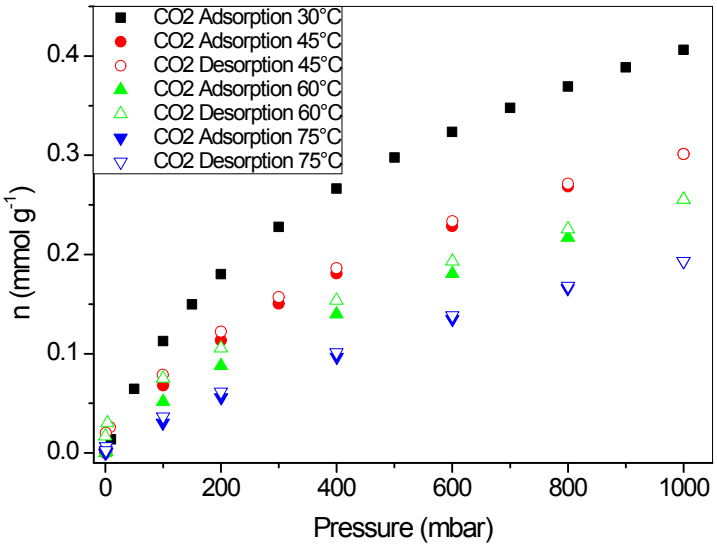

Figure S17 Adsorption/desorption isotherms for CO_2 adsorption on [$Ni_{1.5}$(4,4' bipy)$_{1.5}$(H_3L)] (30 -75°C).

6.3.1 Virial Graphs

(a)

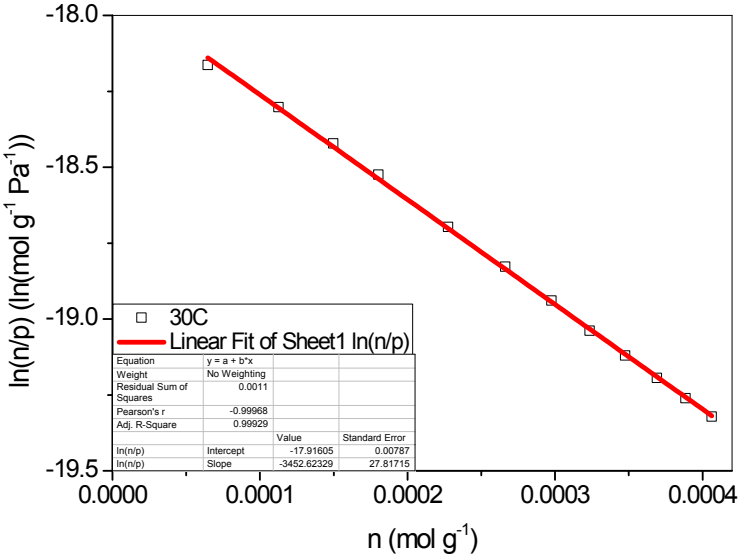

(b)

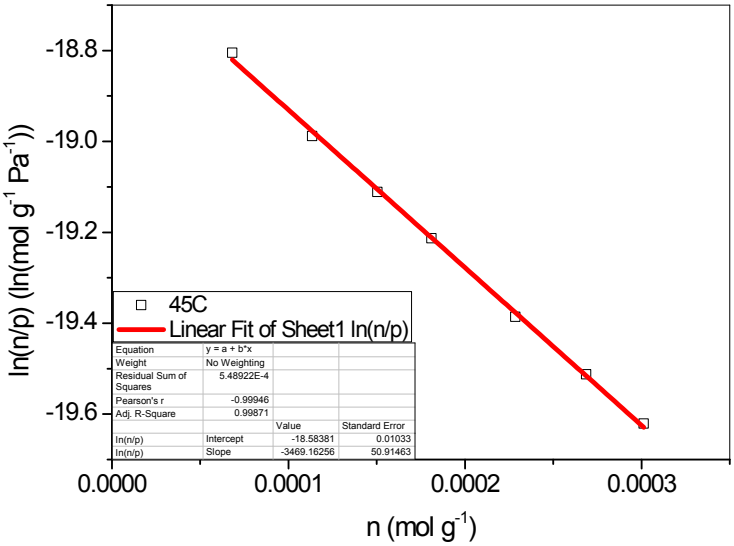
-18.8
-19.0
-19.2
-19.4
-19.6
ln(n/p) (ln(mol g-1 Pa-1))
0.0000
0.0001
0.0002
0.0003
n (mol g-1)
45C
Linear Fit of Sheet1 ln(n/p)
Equation y = a + b*x
Weight No Weighting
Residual Sum of Squares 5.48922E-4
Pearson's r -0.99946
Adj. R-Square 0.99871
Value Standard Error
ln(n/p) Intercept -18.58381 0.01033
ln(n/p) Slope -3469.16256 50.91463

(c)

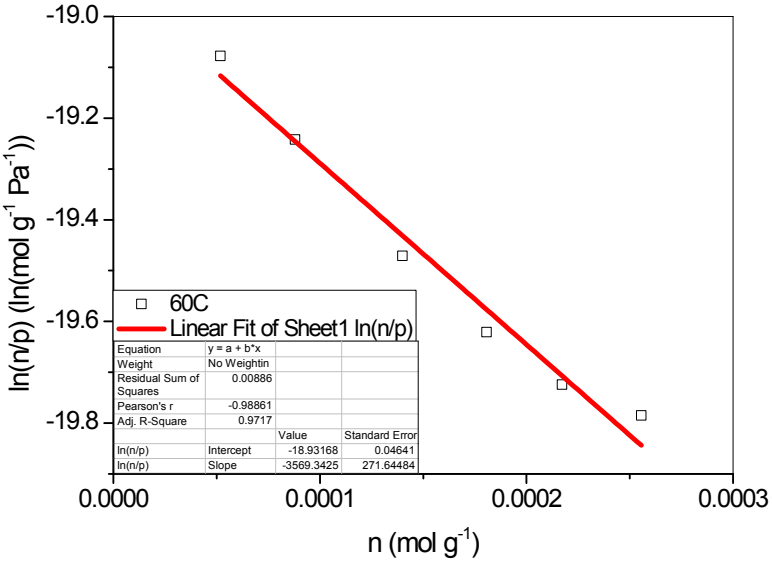
-19.0
-19.2
-19.4
-19.6
-19.8
ln(n/p) (ln(mol g-1 Pa-1))
0.0000
0.0001
0.0002
0.0003
n (mol g-1)
60C
Linear Fit of Sheet1 ln(n/p)
Equation y = a + b*x
Weight No Weightin
Residual Sum of Squares 0.00886
Pearson's r -0.98861
Adj. R-Square 0.9717
Value Standard Error
ln(n/p) Intercept -18.93168 0.04641
ln(n/p) Slope -3569.3425 271.64484

(d)

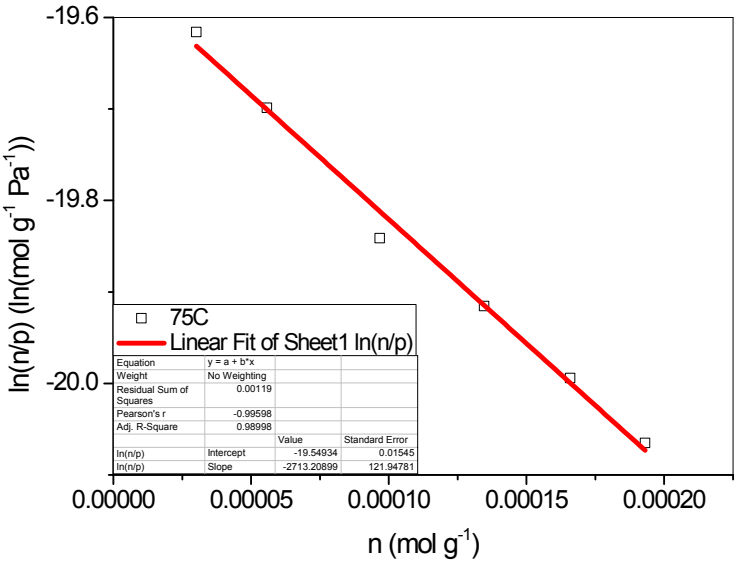

Figure S18. Virial Graphs for Carbon Dioxide Adsorption on $[Ni_{1.5}(4,4'\text{ bipy})_{1.5}(H_3L)]$ at (a) 30°C, (b) 45°C, (c) 60°C and (d) 75°C.

6.3.2 Enthalpy of Adsorption at Zero Surface Coverage

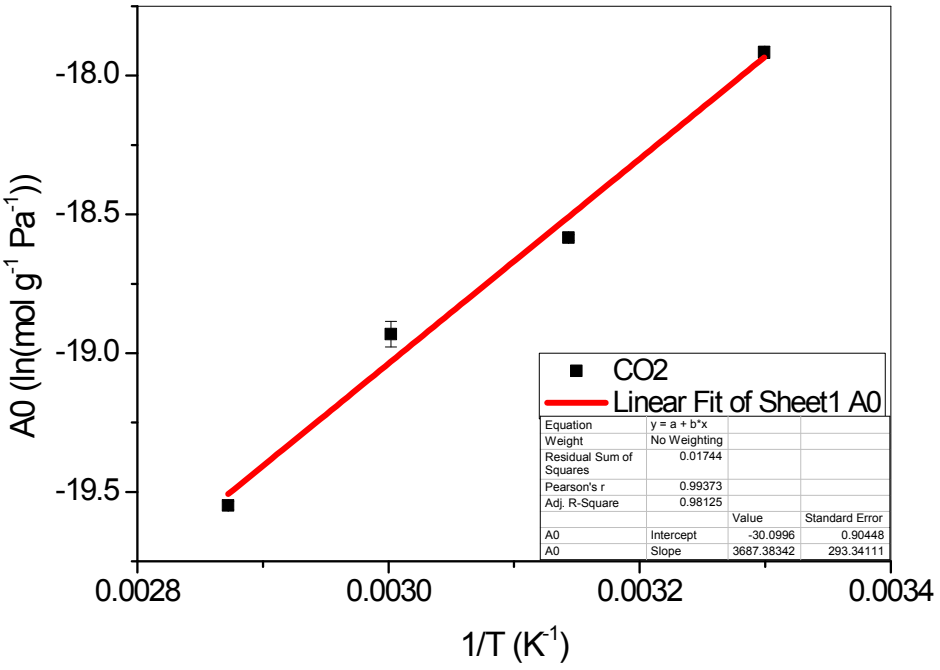

Figure S19. The Variation of Virial Parameter A_0 with 1/T. for Adsorption of CO_2 on $[Ni_{1.5}(4,4'\ bipy)_{1.5}(H_3L)]$.

6.3.3 **Typical Carbon Dioxide Adsorption Kinetic Profiles**

6.3.3.1 Carbon Dioxide Kinetic Profiles for Adsorption at 30°C

(a) 200-300 mbar

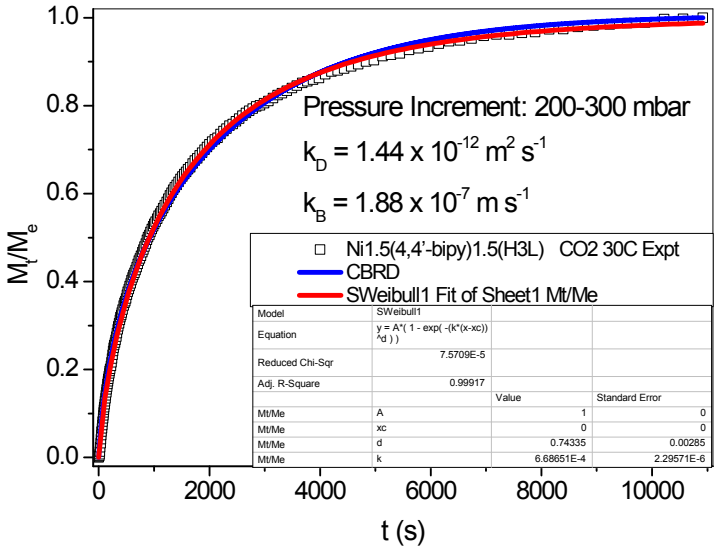

Model	SWeibull1		
Equation	y = A*(1 - exp(-(k*(x-xc)) ^d))		
Reduced Chi-Sqr	7.5709E-5		
Adj. R-Square	0.99917		
		Value	Standard Error
Mt/Me	A	1	0
Mt/Me	xc	0	0
Mt/Me	d	0.74335	0.00285
Mt/Me	k	6.68651E-4	2.29571E-6

(b) 600-700 mbar

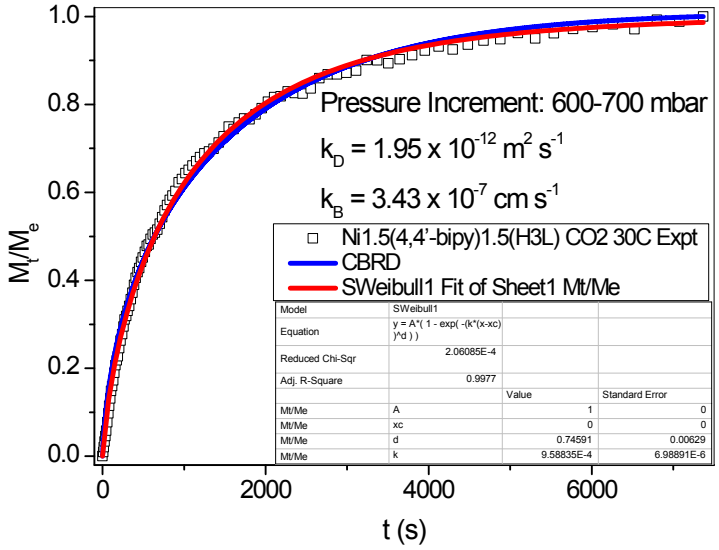

Model	SWeibull1		
Equation	y = A*(1 - exp(-(k*(x-xc))^d))		
Reduced Chi-Sqr	2.06085E-4		
Adj. R-Square	0.9977		
		Value	Standard Error
Mt/Me	A	1	0
Mt/Me	xc	0	0
Mt/Me	d	0.74591	0.00629
Mt/Me	k	9.58835E-4	6.98891E-6

(c) 900-1000 mbar

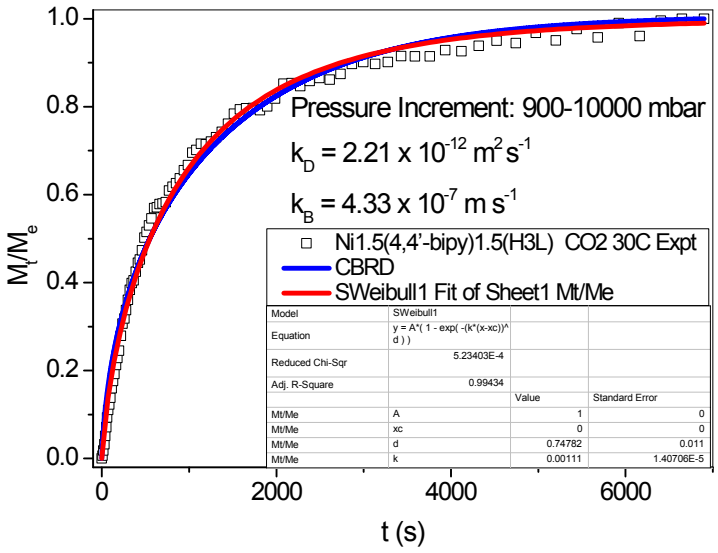

Figure S20. Kinetic Profiles for Adsorption of CO_2 on $[Ni_{1.5}(4,4'\text{ bipy})_{1.5}(H_3L)]$ at 30°C (a) 200-300 mbar, (b) 600-700mbar, (c) 900-1000 mbar.

6.3.3.2 Carbon Dioxide Kinetic Profiles for Adsorption at 45°C

(a) 0-100 mbar

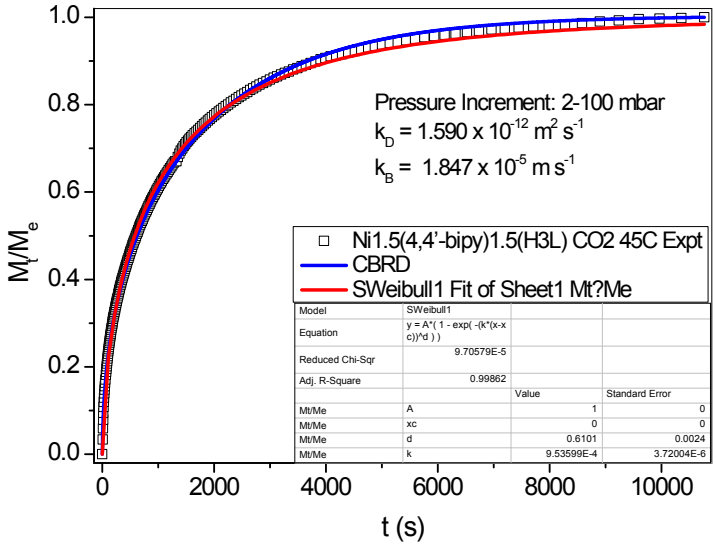

(b) 400-600 mbar

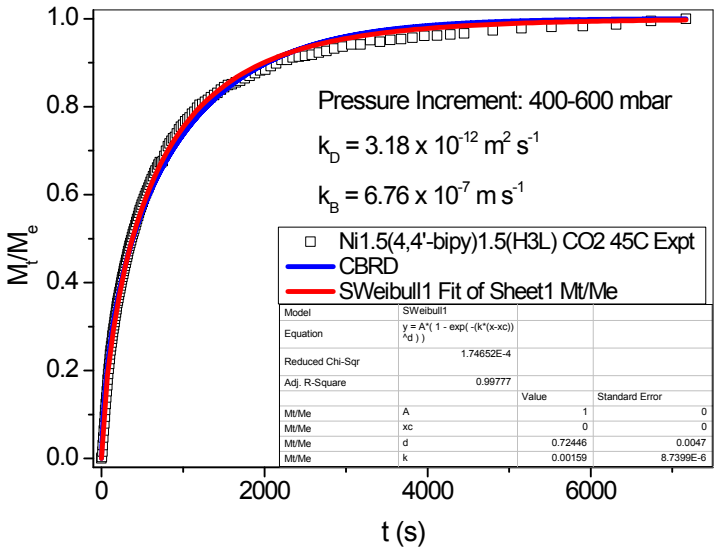

(c) 800-1000 mbar

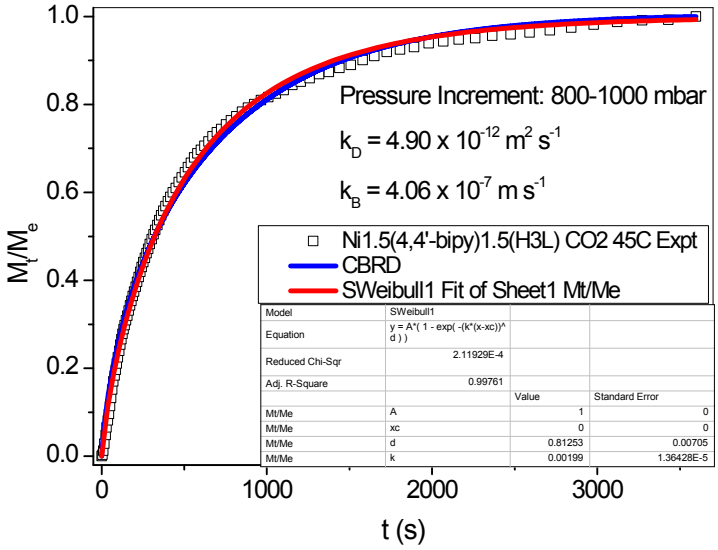

Figure S21. Kinetic Profiles for Adsorption of CO_2 on $[Ni_{1.5}(4,4'\ bipy)_{1.5}(H_3L)]$ at 45°C (a) 0-100 mbar, (b) 400-600 mbar, (c) 800-1000 mbar

6.3.3.3 Carbon Dioxide Kinetic Profiles for Adsorption at 60°C

(a) 0-100 mbar

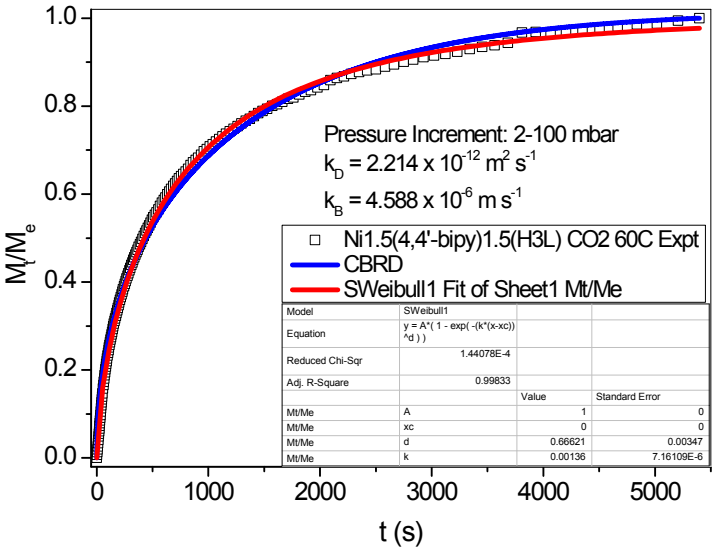

(b) 400-600 mbar

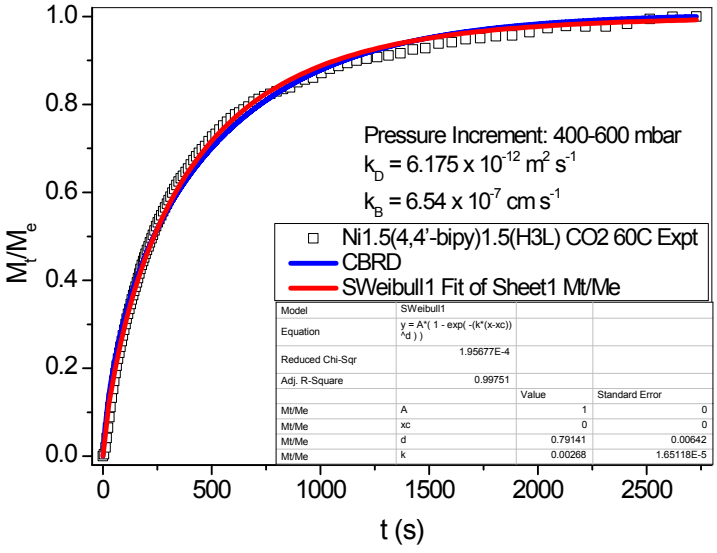

(c) 600-800 mbar

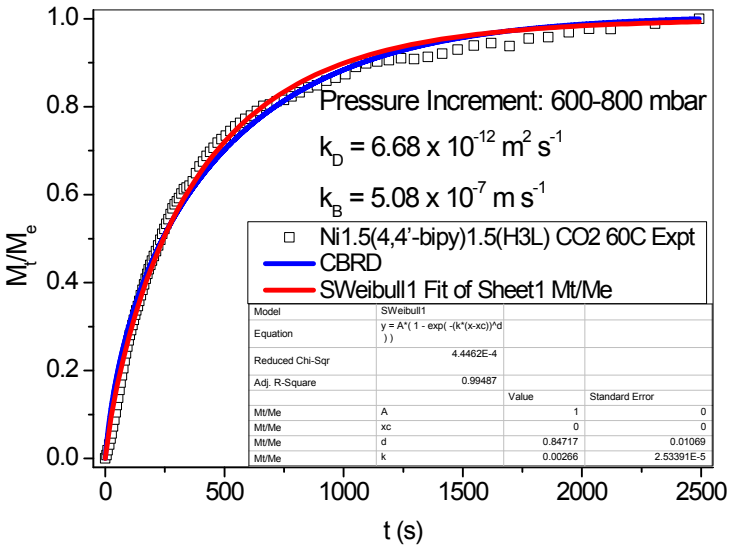

Figure S22. Kinetic Profiles for Adsorption of CO_2 on $[Ni_{1.5}(4,4'\text{ bipy})_{1.5}(H_3L)]$ at 60°C (a) 0-100 mbar, (b) 400-600 mbar, (c) 600-800 mbar.

6.3.3.4 Carbon Dioxide Kinetic Profiles for Adsorption at 75°C

(a) 2-100 mbar

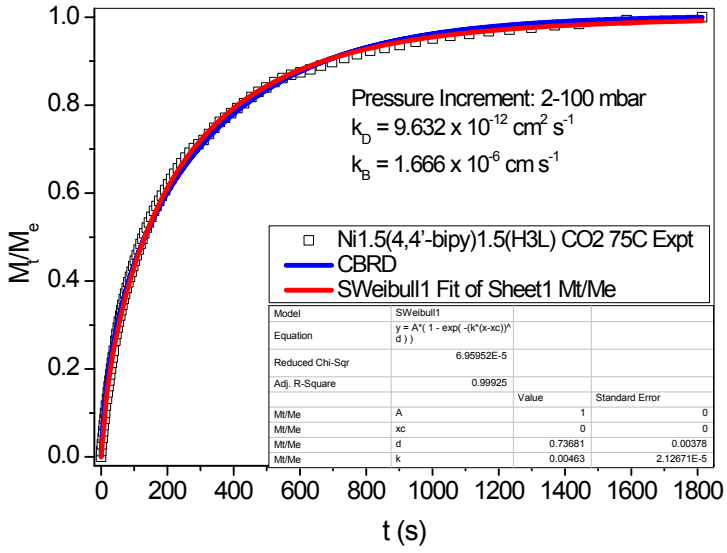

(b) 100-200 mbar

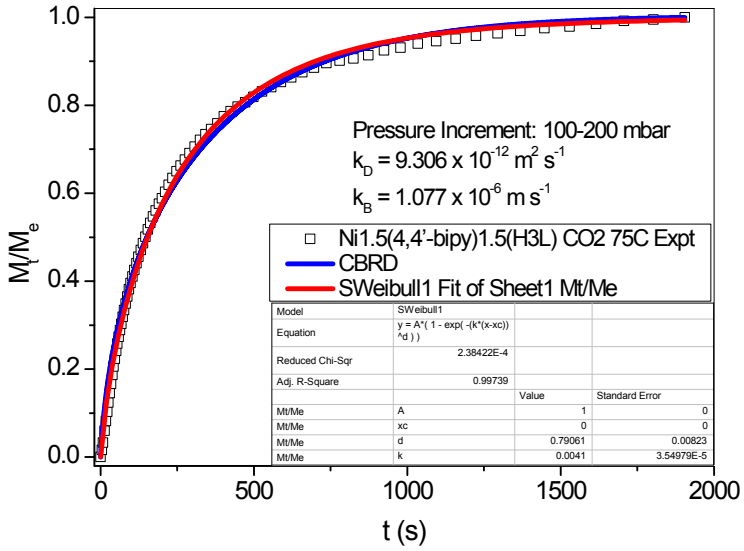

(c) 200-400 mbar

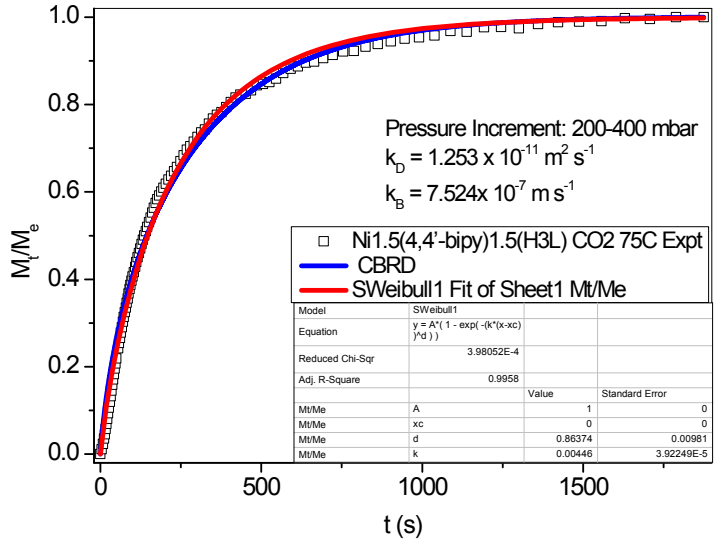

Figure S23. Kinetic Profiles for Adsorption of CO_2 on $[Ni_{1.5}(4,4'\text{ bipy})_{1.5}(H_3L)]$ at 75°C (a) 0-100 mbar, (b) 100-200 mbar, (c) 200-400 mbar.

6.4 Activation Energy Graphs for CO_2 Adsorption on $[Ni_{1.5}(4,4'bipy)_{1.5}(H_3L)]$

(a)

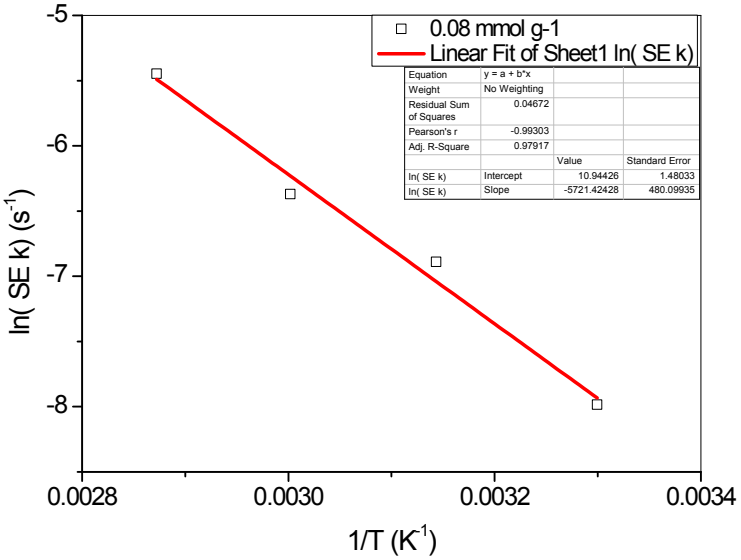

(b)

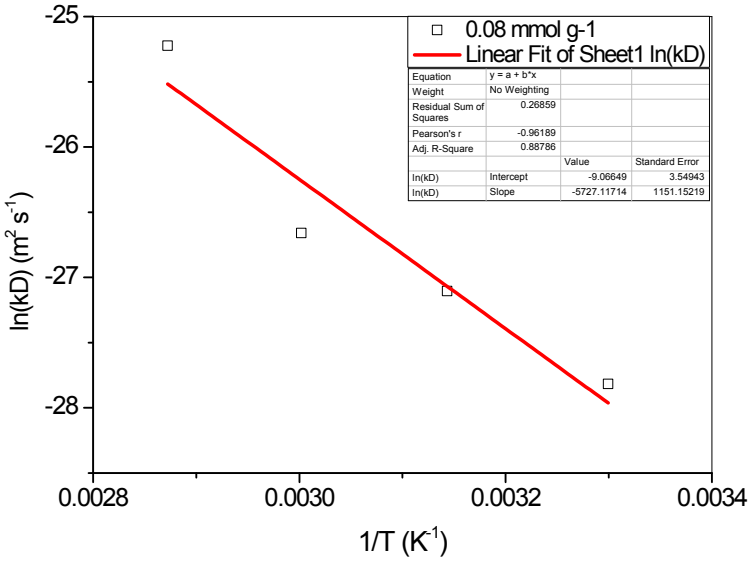

Figure S24 Arrhenius Graphs for CO_2 Adsorption on $[Ni_{1.5}(4,4'bipy)_{1.5}(H_3L)]$ using (a) Stretched Exponential ln(k) and (b) $ln(k_D)$ from the Combined Barrier Resistance Diffusion Model

References.

(1) Van der Made, A. W.; Van der Made, R. H. *The Journal of Organic Chemistry* **1993**, *58*, 1262.
(2) Fawcett, J.; Platt, A. W. G.; Vickers, S. *Polyhedron* **2003**, *22*, 1431.
(3) Murugavel, R.; Singh, M. P. *New J. Chem.* **2010**, *34*, 1846.